

# Outage Performance of Uplink Rate Splitting Multiple Access with Randomly Deployed Users

Huabing Lu, *Student Member, IEEE*, Xianzhong Xie, *Member, IEEE*,  
 Zhaoyuan Shi, *Student Member, IEEE*, Hongjiang Lei, *Senior Member, IEEE*,  
 Nan Zhao, *Senior Member, IEEE*, and Jun Cai, *Senior Member, IEEE*

## Abstract

Rate splitting multiple access (RSMA) is a promising solution to improve spectral efficiency and provide better fairness for the upcoming sixth-generation (6G) networks. In this paper, the outage performance of uplink RSMA transmission with randomly deployed users is investigated, taking both user scheduling schemes and power allocation strategies into consideration. Specifically, the greedy user scheduling (GUS) and cumulative distribution function (CDF) based user scheduling (CUS) schemes are considered, which could maximize the rate performance and guarantee scheduling fairness, respectively. Meanwhile, we re-investigate cognitive power allocation (CPA) strategy, and propose a new rate fairness-oriented power allocation (FPA) strategy to enhance the scheduled users' rate fairness. By employing order statistics and stochastic geometry, an analytical expression of the outage probability for each scheduling scheme combining power allocation is derived to characterize the performance. To get more insights, the achieved diversity order of each scheme is also derived. Theoretical results demonstrate that both GUS and CUS schemes applying CPA or FPA strategy can achieve full diversity orders, and the application of CPA strategy in RSMA can effectively eliminate the secondary user's diversity order constraint from the primary user. Simulation results corroborate the accuracy of the analytical expressions, and show that the proposed FPA strategy can achieve excellent rate fairness performance in high signal-to-noise ratio region.

**Index Terms** —rate splitting multiple access (RSMA), power allocation, user scheduling, outage probability, fairness.

## I. INTRODUCTION

With the rapid development of Internet of Things (IoT), the number of devices required to connect is exploding, which poses a great challenge to the limited available spectrum resource. It is urgent to develop new technologies to improve the spectrum efficiency and connectivity for the next-generation mobile networks. To this end, a novel non-orthogonal transmission

scheme, called rate splitting multiple access (RSMA), has gained significant attention from both academia and industry in recent years [1], [2]. The basic principle of RSMA is to employ rate splitting (RS) at the transmitters, and then apply successive interference cancellation (SIC) at the receivers. Compared with the well-known non-orthogonal multiple access (NOMA) [3], [4], RSMA can manage inter-user interference more flexibly by allowing each user's signal to be partially decoded and partially treated as noise [2], [5]. Taking uplink RSMA as an example, the message of each user is split into two sub-messages at each transmitter, and then one of the sub-messages can be first decoded and eliminated in the SIC. The flexible utilization of RS enables RSMA to achieve the whole capacity region of uplink multiple access channel (MAC) [6]. Comparatively, in the decoding process of NOMA, the signal of one user can be eliminated only after all its messages are successfully decoded, and hence only two corner points of the uplink MAC capacity region are achievable for NOMA [7], [8].

Recently, extensive research attention has been devoted to RSMA transmission. Particularly, in [9], Joudeh *et al.* employed RS to maximize the ergodic sum rate (ESR) of downlink multiple input single output (MISO) system based on partial channel state information (CSI). They showed that in addition to ESR gains, the RSMA can relax CSI quality requirements compared with conventional transmission schemes. Clerckx *et al.* [10] considered a two-user MISO broadcast channel and showed that RSMA can unify orthogonal multiple access (OMA), NOMA, space division multiple access, and multicasting. Considering the power difference constraint of SIC, Yang *et al.* [11] investigated the data rate splitting and power allocation schemes with the objective of maximizing the sum rate of the users. Regarding the uplink transmission, Zeng *et al.* [12] designed a low-complexity algorithm to maximize the minimum data rate of uplink RSMA system and verified its superiority over NOMA. Yang *et al.* [13] investigated the sum rate maximization problem by adjusting users' transmit power and decoding order at the base station (BS).

The aforementioned studies [9]–[13] mainly focused on the design of practical RSMA systems by intelligently optimizing the resource allocation. In order to get some theoretical insights, a number of references dedicated to analyze the performance of RSMA systems. Specifically, Zhu *et al.* [14] first incorporated RS with uplink NOMA and analyzed users' outage performance. Liu *et al.* [15] proposed two kinds of RS schemes to enhance the rate fairness and outage performance of delay-limited uplink RSMA transmissions. In [16], Abbasi *et al.* proposed the cooperative NOMA and cooperative RSMA schemes, and maximized the minimum rates of the two schemes

by considering proportional fairness. Moreover, they also theoretically proved that both schemes can achieve the diversity orders of two. Singh *et al.* [17] studied the outage probability of unmanned aerial vehicle assisted downlink RSMA system, and highlighted the importance of judicious selection of the power allocation coefficients. Kong *et al.* [18] combined RSMA with beamforming to improve the spectral efficiency of satellite system, and analyzed the average throughput performance. Tegos *et al.* [19] presented closed-form expressions for the outage probability of uplink RSMA transmission considering all possible decoding orders. Following the concept of cognitive radio, Liu *et al.* [20] proposed a dynamic power allocation strategy and analyzed the outage performance for uplink RSMA system. More recently, Yue *et al.* [21] proposed two cognitive radio inspired protocols based on RSMA and SIC, and also analyzed the user's outage performance. Note that, fixed user locations were assumed in [14]–[21], which helps to reduce the performance analysis complexity for RSMA transmission. However, in practical systems, user locations are often randomly distributed.

Recently, some studies investigated the performance of downlink RSMA systems by considering the effect of user locations. Specifically, Demarchou *et al.* derived closed-form expressions for the receiver's coverage probability and average sum rate for two-user single input single output (SISO) [22] and MISO [23] downlink RSMA systems. They showed that RSMA brings significant performance gains compared to NOMA. In [24], Demarchou *et al.* proposed a flexible caching-aided RS technique, in which RS is integrated with the caching policies. They considered a single-cell downlink network consisting of several center and edge receivers, and evaluated the achievable rate of each receiver by taking into account the spatial randomness.

Although it has been shown that the application of RSMA for uplink transmission can theoretically achieve the optimal capacity region [6], there is a paucity of literature quantifying the impact of user locations on the performance of uplink RSMA systems. Moreover, the effective user scheduling scheme, which can be applied to enhance the system performance, was not studied in the aforementioned literature [14]–[23]. Furthermore, most of the existing work such as [14], [17]–[19], [22]–[24] studied a fixed power allocation strategy, and the flexibility of RSMA transmission has not been fully explored.

Motivated by these, this paper aims at analyzing the outage performance of uplink RSMA systems with randomly deployed users. In addition, joint effects of both user scheduling schemes and dynamic power allocation strategies are taken into consideration. Furthermore, different from [22]–[25], in which the users are distributed in either the central disc or outer annulus areas, in

this paper, all the users are assumed to be randomly distributed in the disc coverage area of the BS. It should be noted that the performance analysis in this scenario is more complicated, since multi-user scheduling is considered and the scheduled users' channel gains become dependent. The main contributions of this paper are outlined as follows.

- We investigate the performance of uplink RSMA transmission taking into account the effect of random user locations. To effectively utilize the multi-user diversity and achieve the optimal performance, greedy user scheduling (GUS) scheme is employed to select the best users for transmitting. Moreover, in order to address the scheduling fairness issue of the GUS scheme, we invoke cumulative distribution function (CDF) based user scheduling (CUS) to provide fair access opportunities for all users. In addition, based on the stochastic geometry and probability theory, we derive the joint CDF expression of the scheduled users' channel gains for the CUS scheme.
- To fully utilize the flexibility of RSMA, we propose a fairness-oriented power allocation (FPA) strategy to maximize the rate fairness of the scheduled users. We also evaluate the cognitive power allocation (CPA) strategy by taking both user scheduling and spatial randomness into consideration. We theoretically analyze the scheduled users' outage performance for both GUS and CUS schemes combined with both CPA and FPA strategies. Specifically, by applying stochastic geometry and order statistics, we derive analytical expressions for the outage probability of the scheduled users. To get more insights, we also analyze the users' achievable diversity orders under these different scenarios.
- Through sufficient theoretical analyses and simulation results, we demonstrate that both scheduling schemes can achieve full diversity orders with each power allocation strategy. Moreover, we illustrate that the secondary user's achievable diversity order for the CPA strategy is not restricted by the primary user's channel quality in the RSMA transmission. In addition, we show that the application of FPA strategy to RSMA can achieve rate fairness in high signal-to-noise ratio (SNR) region, and hence the combination of CUS scheme with FPA strategy can achieve both scheduling fairness and rate fairness in the RSMA transmission.

The rest of this paper is organized as follows. Section II introduces the system model. The power allocation strategies, scheduling schemes and the corresponding scheduled users' channel gains' joint distribution functions are provided in Section III. Sections IV and V analyze the outage performance of CPA and FPA strategies, respectively. In Section VI, simulation results are presented to corroborate the theoretical analyses, and Section VII concludes this paper.

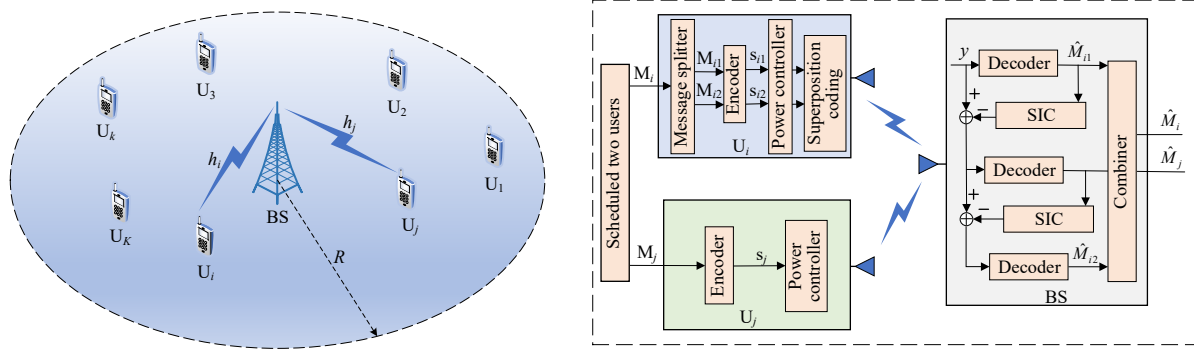


Fig. 1. Then considered system model and transceiver architecture of 2-user uplink RSMA.

## II. SYSTEM MODEL

As shown in Fig. 1, we consider a single-cell uplink cellular network, where a single-antenna BS is located at the center of the coverage disc area with radius  $R$ . There are  $K$  single-antenna users, denoted as  $U_k$ ,  $k = 1, 2, \dots, K$ , randomly distributed in the coverage area of the BS, following a homogeneous Binomial point process (HBPP)  $\Upsilon_B$  [26]. The time is slotted into intervals of equal length. At the beginning of each time slot, every user can estimate its CSI based on the pilots sent by the BS.

The channel between the  $k$ -th user  $U_k$  and the BS is modeled as  $h_k = \frac{\iota_k}{\sqrt{1+r_k^\alpha}}$ , where  $r_k$  represents the distance between  $U_k$  and the BS,  $\alpha$  denotes the path-loss exponent, and  $\iota_k$  represents Rayleigh fading coefficient with  $\iota_k \sim \mathcal{CN}(0, 1)$ . The channel coefficients are assumed to be invariant in each time slot but can change independently among slots. Without loss of generality, we assume that the users' channel gains are ordered as

$$|h_1|^2 \geq \dots \geq |h_K|^2. \quad (1)$$

In each time slot, two of the  $K$  users, denoted as  $U_i$  and  $U_j$ , are scheduled to communicate with the BS. In the uplink RSMA, it has been shown that a single user's signal splitting can guarantee the system to achieve the whole capacity region of uplink MAC [6], [7]. Hence, we assume that the message of  $U_i$ ,  $M_i$ , is split into two sub-messages  $M_{i1}$  and  $M_{i2}$ . The two sub-messages are independently encoded into streams  $s_{i1}$  and  $s_{i2}$ . Then, the two streams are allocated with certain powers and superposed at  $U_i$ . Thus, the received signal at the BS can be expressed as

$$y = \sqrt{\beta P_i} h_i s_{i1} + \sqrt{(1-\beta) P_i} h_i s_{i2} + \sqrt{P_j} h_j s_j + n_0, \quad (2)$$

where  $s_v$ ,  $v \in \{i1, i2, j\}$ , satisfies  $\mathbb{E}[|s_v|^2] = 1$ ,  $P_i$  ( $P_j$ ) represents the transmit power of  $s_{i1}$  ( $s_{i2}$ ),  $\beta$  ( $0 \leq \beta \leq 1$ ) denotes the power allocation coefficient of  $U_i$ , and  $n_0$  represents the additive white Gaussian noise (AWGN) at the BS with zero mean and variance  $\sigma^2$ . For ease of representation,

in the rest of the paper, we denote the transmit SNR of  $U_i$  ( $U_j$ ) as  $\rho_i = \frac{P_i}{\sigma^2}$  ( $\rho_j = \frac{P_j}{\sigma^2}$ ), and use  $\eta_i = \rho_i|h_i|^2$  ( $\eta_j = \rho_j|h_j|^2$ ) to represent the effective received SNRs of  $U_i$  ( $U_j$ ). Assume that all users have the same maximal transmit SNR  $\rho_m$ .

The transceiver architecture of a 2-user uplink RSMA is illustrated in Fig. 1, and SIC is executed at the BS to decode the transmitted messages. In this paper, we assume that the decoding order is  $s_{i1} \rightarrow s_j \rightarrow s_{i2}$  as in [15]. Particularly, if  $\beta = 0$  ( $\beta = 1$ ), the RSMA transmission will degrade to NOMA transmission, and the decoding order will become  $s_j \rightarrow s_i$  ( $s_i \rightarrow s_j$ ). Based on (2), the instantaneous signal to interference plus noise ratio (SINR) for decoding  $s_{i1}$  can be denoted as

$$\text{SINR}_{i1} = \frac{\beta \rho_i |h_i|^2}{(1 - \beta) \rho_i |h_i|^2 + \rho_j |h_j|^2 + 1}. \quad (3)$$

If  $s_{i1}$  can be successfully decoded, it will be reconstructed and eliminated from the compound signal. Then the remaining signal can be represented as

$$\tilde{y} = \sqrt{(1 - \beta) P_i} h_i s_{i2} + \sqrt{P_j} h_j s_j + n_0. \quad (4)$$

From (4), the SINR for decoding  $s_j$  can be expressed as

$$\text{SINR}_j = \frac{\rho_j |h_j|^2}{(1 - \beta) \rho_i |h_i|^2 + 1}. \quad (5)$$

Similarly, if  $s_j$  is correctly decoded, the SNR of decoding  $s_{i2}$  can be denoted as

$$\text{SINR}_{i2} = (1 - \beta) \rho_i |h_i|^2. \quad (6)$$

In this paper, outage probability is used as the performance metric, which is defined as the probability that the instantaneous achievable rate of a user is less than a target one. To gain more insights, diversity order will also be derived. The diversity order highlights the scaling law of the outage probability with respect to the transmit SNR, which can be defined as [27]

$$d = - \lim_{\rho \rightarrow \infty} \frac{\log \mathcal{P}(\rho)}{\log \rho}, \quad (7)$$

where  $\mathcal{P}(\rho)$  and  $\rho$  denote the outage probability and transmit SNR, respectively.

### III. SCHEDULING SCHEMES AND POWER ALLOCATION STRATEGIES

In this section, the GUS and CUS schemes are first presented, and the joint CDFs of the scheduled users' channel gains are given. Then, the CPA and FPA strategies are introduced.

#### A. Scheduling Schemes

Two scheduling schemes are investigated in this paper. In particular, the GUS scheme is first considered in order to maximize the system performance. Then, CUS scheme is introduced to tackle the scheduling fairness problem of the GUS scheme, which can also effectively utilize the multi-user diversity gain.

1) *GUS Scheme*: In the GUS scheme, two users with the largest channel gains, namely,  $U_1$  and  $U_2$ , are scheduled, and the joint probability density function (PDF) of their channel gains is [28]

$$f_{|h_2|^2, |h_1|^2}^{\text{GUS}}(x, y) = K(K-1)f_{|h|^2}(x)f_{|h|^2}(y)F_{|h|^2}(x)^{K-2}, \quad (8)$$

where  $x \leq y$ .  $F_{|h|^2}(x)$  and  $f_{|h|^2}(x)$  respectively represent the CDF and PDF of the randomly selected user's channel gain. According to [29], we have

$$F_{|h|^2}(x) \approx \sum_{l=1}^L \Psi_l (1 - e^{-\mu_l x}), \quad (9)$$

and

$$f_{|h|^2}(x) \approx \sum_{l=1}^L \Psi_l \mu_l e^{-\mu_l x}, \quad (10)$$

where  $\psi_l = \cos\left(\frac{2l-1}{2L}\pi\right)$ ,  $\mu_l = 1 + \left(\frac{D_F}{2} + \frac{D_F}{2}\psi_l\right)^\alpha$ ,  $\Psi_l = \frac{\pi}{L}\sqrt{1-\psi_l^2}(1+\psi_l)$ , and  $L$  is the parameter to make the tradeoff between complexity and accuracy.

It is intuitional that the GUS scheme can achieve the best rate performance, since it always schedules the users with the largest channel gains. However, as the users closer to the BS have smaller path losses and then are scheduled more often than others, the scheduling fairness issue arises. In the following, CUS is invoked to provide fair scheduling opportunities for the users.

2) *CUS Scheme*: In CUS scheme, the two users with the largest CDF values with respect to their channel gains, namely, the users whose channels are good enough relative to their own statistics [25], [30], will be selected to transmit. Assume that the CDF of  $U_k$ 's channel gain  $|h_k|^2$  is denoted as  $F_k(x)$ , which can be obtained by the user's observation [31]. In this paper, we use "CDF" to denote the cumulative distribution function, for example,  $F_k(x)$ , and use "CDF value" to represent the corresponding output value of a CDF with a specific input  $x$ . Every user can get its channel gain's CDF value at the beginning of each time slot.

For Rayleigh small-scale fading, the CDF of  $U_k$ 's channel gain with a given distance  $r_k$  can be expressed as

$$F_k(x|r_k) = 1 - e^{-(1+r_k^\alpha)x}. \quad (11)$$

Let  $\mathcal{U}_k = F_k(x|r_k)$ . Since the user's channel gain is a random variable,  $\mathcal{U}_k$  is a random variable as well. According to [31],  $\mathcal{U}_k$  is uniformly distributed in  $[0, 1]$ . Moreover, since all users' channels are assumed to be independent of each other, every user has the same probability to have the largest CDF value and hence the scheduling fairness can be guaranteed [30], [31]. The joint CDF of the two users' channel gains in CUS scheme is given in the following lemma.

*Lemma 1:* Let random variables  $X$  and  $Y$  denote the channel gains of users with the largest and the second-largest CDF values, respectively. Then, the joint CDF of  $X$  and  $Y$  in CUS scheme can be approximated as the following 4 cases.

Case 1: If  $x \geq (R^\alpha + 1)y$ ,

$$\begin{aligned} F_{X,Y}^{\text{CUS}}(x, y) \approx & K \sum_{l_1=1}^L \Psi_{l_1} (1 - e^{-\mu_{l_1} y})^{K-1} \sum_{l_2=1}^L \Psi_{l_2} (1 - e^{-\mu_{l_2} x}) \\ & - (K-1) \sum_{l_1=1}^L \Psi_{l_1} (1 - e^{-\mu_{l_1} y})^K. \end{aligned} \quad (12)$$

Case 2: If  $y \leq x < (R^\alpha + 1)y$ ,

$$\begin{aligned} F_{X,Y}^{\text{CUS}}(x, y) \approx & K a_1 w_M \sum_{m=1}^M t_m [1 - e^{-(1+t_m^\alpha)y}]^{K-1} \sum_{l=1}^L \Psi_l (1 - e^{-\mu_l x}) \\ & + K(R - a_1) w_Q \sum_{q=1}^Q \Theta_q [1 - e^{-(1+\Theta_q^\alpha)y}]^{K-1} (R - I_1(\Theta_q)) \\ & \times w_N \sum_{n=1}^N \Phi_n(\Theta_q) [1 - e^{-(1+\Phi_n(\Theta_q)^\alpha)x}] \\ & - (K-1)a_1 w_M \sum_{m=1}^M t_m [1 - e^{-(1+t_m^\alpha)y}]^K \\ & - (K-1)(R - a_1) w_Q \sum_{q=1}^Q \Theta_q [1 - e^{-(1+\Theta_q^\alpha)y}]^K [1 - \frac{1}{R^2} I_1(\Theta_q)^2] \\ & + a_2 w_B \sum_{b=1}^B \Xi_b [1 - e^{-(1+\Xi_b^\alpha)x}]^K [1 - \frac{1}{R^2} I_2(\Xi_b)^2]. \end{aligned} \quad (13)$$

Case 3: If  $x < y < (R^\alpha + 1)x$ ,

$$\begin{aligned} F_{X,Y}^{\text{CUS}}(x, y) \approx & K a_2 w_B \sum_{b=1}^B \Xi_b [1 - e^{-(1+\Xi_b^\alpha)y}]^{K-1} \\ & \times (R - I_1(\Xi_b)) w_N \sum_{n=1}^N \Phi_n(\Xi_b) [1 - e^{-(1+\Phi_n(\Xi_b)^\alpha)x}] \\ & - (K-1)a_2 w_B \sum_{b=1}^B \Xi_b [1 - e^{-(1+\Xi_b^\alpha)y}]^K [1 - \frac{1}{R^2} I_1(\Xi_b)^2] \\ & + a_1 w_M \sum_{m=1}^M t_m [1 - e^{-(1+t_m^\alpha)x}]^K \\ & + (R - a_1) w_Q \sum_{q=1}^Q \Theta_q [1 - e^{-(1+\Theta_q^\alpha)x}]^K [1 - \frac{1}{R^2} I_2(\Theta_q)^2]. \end{aligned} \quad (14)$$

Case 4: If  $y \geq (R^\alpha + 1)x$ ,

$$F_{X,Y}^{\text{CUS}}(x, y) \approx \sum_{l=1}^L \Psi_l (1 - e^{-\mu_l x})^K. \quad (15)$$

Where, if  $x \geq y$ ,  $a_1 = (\frac{x}{y} - 1)^{\frac{1}{\alpha}}$ ,  $a_2 = [\frac{y}{x}(R^\alpha + 1) - 1]^{\frac{1}{\alpha}}$ ; if  $y > x$ ,  $a_1 = (\frac{y}{x} - 1)^{\frac{1}{\alpha}}$ ,  $a_2 = [\frac{x}{y}(R^\alpha + 1) - 1]^{\frac{1}{\alpha}}$ .  $I_1(z) = [\frac{y}{x}(1 + z^\alpha) - 1]^{\frac{1}{\alpha}}$ ,  $I_2(z) = [\frac{x}{y}(1 + z^\alpha) - 1]^{\frac{1}{\alpha}}$ ,  $w_M = \frac{\pi}{MR^2} \sqrt{1 - \varphi_m^2}$ ,  $\varphi_m = \cos(\frac{2m-1}{2M}\pi)$ ,  $t_m = \frac{a_1}{2}(1 + \varphi_m)$ ,  $w_Q = \frac{\pi}{QR^2} \sqrt{1 - \theta_q^2}$ ,  $\theta_q = \cos(\frac{2q-1}{2Q}\pi)$ ,  $\Theta_q = \frac{R+a_1}{2} - \frac{R-a_1}{2}\theta_q$ ,  $w_N = \frac{\pi}{NR^2} \sqrt{1 - \phi_n^2}$ ,  $\phi_n = \cos(\frac{2n-1}{2N}\pi)$ ,  $\Phi_n(z) = \frac{R+I_1(z)}{2} + \frac{R-I_1(z)}{2}\phi_n$ ,  $w_B = \frac{\pi}{BR^2} \sqrt{1 - \xi_b^2}$ ,  $\xi_b = \cos(\frac{2b-1}{2B}\pi)$ ,  $\Xi_b = \frac{a_2}{2}(1 + \xi_b)$ ,  $M$ ,  $Q$ ,  $N$ , and  $B$  are parameters for complexity-accuracy trade-off.

*Proof:* Please refer to Appendix A. ■

*Remark 1:* It can be seen from Lemma 1 that the parameters  $R$  and  $\alpha$  as well as the values of  $X$  and  $Y$  have an essential impact on the expression of the joint CDF. Because of this, calculating the outage probability of the CUS scheme is quite involved.

When  $y \geq (R^\alpha + 1)x$ , we know from (15) that the joint CDF is only related to the channel gain of the user with the largest CDF value. Actually, (15) also represents the channel gain's CDF of this user. By applying the joint CDF in (12), when  $x \rightarrow \infty$ , we can obtain the CDF of channel gain for the user with the second-largest CDF value as

$$F_Y^{\text{CUS}}(y) \approx K \sum_{l_1=1}^L \Psi_{l_1} (1 - e^{-\mu_{l_1} y})^{K-1} - (K-1) \sum_{l_1=1}^L \Psi_{l_1} (1 - e^{-\mu_{l_1} y})^K. \quad (16)$$

## B. Power Allocation Strategies

In this paper, we consider two dynamic power allocation strategies, where the CPA strategy intends to prioritize the quality of service (QoS) of one user, while the FPA strategy aims to maximize the scheduled users' rate fairness performance.

1) *CPA Strategy:* In CPA strategy [20], [21], [32], one of the scheduled two users is deemed as primary user (denoted as  $U_p$ ), and the other user is regarded as secondary user (denoted as  $U_s$ ). Particularly, the QoS of  $U_p$  should be satisfied with priority, while  $U_s$  can be served on the premise that its access can not affect the performance of  $U_p$ . Hence, compared with the conventional OMA transmission in which the spectrum is solely occupied by one user, applying CPA strategy in RSMA can greatly enhance the connectivity and improve the spectrum efficiency. In order not to affect the transmission of  $U_p$ ,  $U_s$  is deemed as the splitting-user (namely, its message may be split into two parts). Based on the instantaneous channel gains of the scheduled users, the CPA strategy is designed with the following three cases [20], [21]:

- 1) The signal of  $U_p$  cannot be successfully decoded even if it solely occupies the channel, i.e.,  $\log_2(1 + \eta_p) < \hat{R}_p$ , where  $\eta_p = \rho_p |h_p|^2$  and  $\hat{R}_p$  denotes the target data rate of  $U_p$ : In this case,  $U_p$  will be in an outage definitely. In order to maximize  $U_s$ 's data rate, the power allocation coefficient  $\beta$  should be set as 1 to make  $U_s$ 's signal be decoded at the first stage of SIC. Hence,  $U_s$  should not be split, and its achievable rate is  $\log_2\left(1 + \frac{\eta_s}{\eta_p + 1}\right)$ , where  $\eta_s = \rho_s |h_s|^2$ .
- 2) The signal of  $U_p$  can be successfully decoded even if all the received power of  $U_s$  is regarded as noise, namely,  $\log_2\left(1 + \frac{\eta_p}{\eta_s + 1}\right) \geq \hat{R}_p$ : In this case, to maximize the performance of  $U_s$ ,  $\beta$  should be set as 0, and the achievable rate of  $U_s$  is  $\log_2(1 + \eta_s)$ .
- 3) The signal of  $U_p$  can be successfully decoded if it solely occupies the channel, but cannot be decoded if all the received power of  $U_s$  is regarded as noise, i.e.,  $\log_2(1 + \eta_p) \geq \hat{R}_p$  and  $\log_2\left(1 + \frac{\eta_p}{\eta_s + 1}\right) < \hat{R}_p$ : In this case, RS should be conducted at  $U_s$ . Specifically, in order to guarantee the QoS of  $U_p$  and to maximize the achievable data rate of  $U_s$ ,  $\beta$  should be set to meet  $\log_2\left(1 + \frac{\eta_p}{(1-\beta)\eta_s + 1}\right) = \hat{R}_p$ , namely,  $\beta = 1 - \frac{\eta_p - \hat{\gamma}_p}{\eta_s \hat{\gamma}_p}$ , where  $\hat{\gamma}_p = 2^{\hat{R}_p} - 1$ . According to (3) and (6), the achievable data rate of  $U_s$  is  $\log_2\left(\frac{\hat{\gamma}_p(1 + \eta_p + \eta_s)}{\eta_p(1 + \hat{\gamma}_p)}\right) + \log_2\left(\frac{\eta_p}{\hat{\gamma}_p}\right) = \log_2(1 + \eta_p + \eta_s) - \hat{R}_p$ .

2) *FPA Strategy*: We propose FPA strategy to fully utilize the flexibility of RSMA to improve the scheduled users rate fairness. It has been shown that two corner points on the capacity region of uplink MAC can be achieved by NOMA transmission [7], i.e.,  $(R_i^F, R_j^S)$  and  $(R_i^S, R_j^F)$ , where  $R_i^F = \log(1 + \frac{\eta_i}{1 + \eta_j})$  and  $R_i^S = \log(1 + \eta_i)$  denote the achievable rates of decoding  $U_i$ 's signal at the first and second stages of SIC, respectively. In addition to these two corner points, RSMA transmission can achieve all the points on the line of the two corner points by adjusting the power allocation factor  $\beta$ , where all these points can achieve the same sum rate performance [6], [14], [15]. In other words, by using RSMA, the sum rate  $R_i^F + R_j^S = \log_2(1 + \eta_i + \eta_j)$  can be flexibly allocated to the scheduled users by adjusting  $\beta$ . Hence, we utilize this feature to enhance the scheduled users' rate fairness performance on the premise of achieving the optimal sum rate.

Assuming  $\eta_i > \eta_j$ , we know rate-pair  $(R_i^F, R_j^S)$  can achieve much better rate fairness than  $(R_i^S, R_j^F)$ , since the first decoded user's achievable data rate will be interfered by the second decoded user's signal. Furthermore, if  $R_i^F \geq R_j^S$ , both NOMA and RSMA schemes can achieve the same fairness performance by setting  $\beta = 0$  and decoding  $U_i$ 's signal at the first stage of SIC. In other words, when  $\log_2\left(1 + \frac{\eta_i}{\eta_j + 1}\right) \geq \log_2(1 + \eta_j)$  (i.e.,  $\eta_i \geq \eta_j + \eta_j^2$ ), the data rates of

$U_i$  and  $U_j$  are  $\log_2 \left(1 + \frac{\eta_i}{\eta_j + 1}\right)$  and  $\log_2 (1 + \eta_j)$ , respectively.

On the other hand, if  $R_i^F < R_j^S$  (i.e.,  $\eta_i < \eta_j + \eta_j^2$ ), RSMA can achieve better fairness than NOMA. Then, by applying proper power allocation strategy to  $U_j$ , the scheduled users can achieve the same data rate, namely,  $R_i = R_j = \frac{1}{2} \log_2 (1 + \eta_i + \eta_j)$ . By setting  $\log_2 \left(1 + \frac{\eta_i}{(1-\beta)\eta_j + 1}\right) = \frac{1}{2} \log_2 (1 + \eta_i + \eta_j)$ , the power allocation coefficient can be derived as  $\beta = 1 + \frac{1}{\eta_j} - \frac{\eta_i}{\eta_j (\sqrt{1 + \eta_j + \eta_j} - 1)}$ . As such, the transmission rates of  $U_{j1}$  and  $U_{j2}$  are  $\log_2 \left(1 + \frac{\beta \eta_j}{(1-\beta)\eta_j + \eta_j + 1}\right)$  and  $\log_2 (1 + (1-\beta)\eta_j)$ , respectively. Hence, in the case  $\eta_i > \eta_j$ , the power allocation coefficient of the splitting-user  $U_j$  is

$$\beta = \begin{cases} 0, & \text{if } \eta_i \geq \eta_j + \eta_j^2 \\ 1 + \frac{1}{\eta_j} - \frac{\eta_i}{\eta_j (\sqrt{1 + \eta_j + \eta_j} - 1)}, & \text{otherwise} \end{cases}. \quad (17)$$

For the case  $\eta_i \leq \eta_j$ ,  $U_i$  is regarded as the splitting-user, and the power allocation coefficient can be derived similar to the case  $\eta_i > \eta_j$ .

#### IV. OUTAGE PERFORMANCE ANALYSIS OF THE CPA STRATEGY

In this section, the outage probability framework of CPA strategy is derived first. Then, the outage performance of the GUS and CUS scheme with CPA strategy is analyzed.

##### A. Outage Probability of the CPA Strategy

In CPA strategy, as  $U_p$  can achieve the same performance as that achieved in OMA transmission, we only evaluate the outage performance of  $U_s$  [32], which can be expressed as

$$\begin{aligned} \mathcal{P}^{\text{CPA}} = & \mathbb{P} \left[ \log_2 (1 + \eta_p) \leq \hat{R}_p, \log_2 \left(1 + \frac{\eta_s}{\eta_p + 1}\right) < \hat{R}_s \right] \\ & + \mathbb{P} \left[ \log_2 \left(1 + \frac{\eta_p}{\eta_s + 1}\right) > \hat{R}_p, \log_2 (1 + \eta_s) < \hat{R}_s \right] \\ & + \mathbb{P} \left[ \log_2 (1 + \eta_p) > \hat{R}_p, \log_2 \left(1 + \frac{\eta_p}{\eta_s + 1}\right) < \hat{R}_p, \right. \\ & \quad \left. \log_2 (1 + \eta_p + \eta_s) - \hat{R}_p < \hat{R}_s \right], \end{aligned} \quad (18)$$

where  $\hat{R}_s$  denotes the target data rate of  $U_s$ . The first term denotes both  $U_p$  and  $U_s$  are in outage (in this case  $\beta = 1$ , namely,  $U_s$ 's signal is decoded at the first stage of SIC). The second term represents that  $U_p$ 's signal is successfully decoded at the first stage of SIC, and  $U_s$ 's signal is in an outage (in this case  $\beta = 0$ ). The third term shows that  $U_p$ 's signal can be successfully decoded at the second stage of SIC, but  $U_s$  is still in an outage (in this case  $0 < \beta < 1$ ).

After some manipulations, (18) can be expressed as

$$\begin{aligned}\mathcal{P}^{\text{CPA}} = & \mathbb{P}\left[\frac{\eta_s}{\hat{\gamma}_s} - 1 < \eta_p \leq \hat{\gamma}_p\right] + \mathbb{P}[\eta_p > \hat{\gamma}_p(\eta_s + 1), \eta_s < \hat{\gamma}_s] \\ & + \mathbb{P}[\hat{\gamma}_p < \eta_p < \hat{\gamma}_p(\eta_s + 1), \eta_p < \hat{\gamma}_p + \hat{\gamma}_s + \hat{\gamma}_p\hat{\gamma}_s - \eta_s],\end{aligned}\quad (19)$$

where  $\hat{\gamma}_s = 2^{\hat{R}_s} - 1$  and  $\hat{\gamma}_p + \hat{\gamma}_s + \hat{\gamma}_p\hat{\gamma}_s = 2^{\hat{R}_p + \hat{R}_s} - 1$  is applied. With some manipulations, we find that the first term in (19) holds if  $\eta_s < \hat{\gamma}_s(1 + \hat{\gamma}_p)$ . For the third term in (19), we know that  $\hat{\gamma}_p(\eta_s + 1) < \hat{\gamma}_p + \hat{\gamma}_s + \hat{\gamma}_p\hat{\gamma}_s - \eta_s$  holds if  $\eta_s < \hat{\gamma}_s$ , and vice versa. Hence, (19) can be converted to

$$\begin{aligned}\mathcal{P}^{\text{CPA}} = & \mathbb{P}\left[\frac{\eta_s}{\hat{\gamma}_s} - 1 < \eta_p \leq \hat{\gamma}_p, \eta_s < \hat{\gamma}_s(1 + \hat{\gamma}_p)\right] + \mathbb{P}[\eta_p > \hat{\gamma}_p(\eta_s + 1), \eta_s < \hat{\gamma}_s] \\ & + \mathbb{P}[\hat{\gamma}_p < \eta_p < \hat{\gamma}_p(\eta_s + 1), \eta_s < \hat{\gamma}_s] \\ & + \mathbb{P}[\hat{\gamma}_p < \eta_p < \hat{\gamma}_p + \hat{\gamma}_s + \hat{\gamma}_p\hat{\gamma}_s - \eta_s, \eta_s > \hat{\gamma}_s].\end{aligned}\quad (20)$$

To guarantee  $\hat{\gamma}_p < \hat{\gamma}_p + \hat{\gamma}_s + \hat{\gamma}_p\hat{\gamma}_s - \eta_s$  in the fourth term of (20),  $\eta_s$  should be less than  $\hat{\gamma}_s(1 + \hat{\gamma}_p)$ . Based on that, and combining the second and third terms of (20), the outage probability for the CPA strategy can be further denoted as

$$\begin{aligned}\mathcal{P}^{\text{CPA}} = & \mathbb{P}\left[\frac{\eta_s}{\hat{\gamma}_s} - 1 < \eta_p \leq \hat{\gamma}_p, \eta_s < \hat{\gamma}_s(1 + \hat{\gamma}_p)\right] + \mathbb{P}[\eta_p > \hat{\gamma}_p, \eta_s < \hat{\gamma}_s] \\ & + \mathbb{P}[\hat{\gamma}_p < \eta_p < \hat{\gamma}_p + \hat{\gamma}_s + \hat{\gamma}_p\hat{\gamma}_s - \eta_s, \hat{\gamma}_s < \eta_s < \hat{\gamma}_s(1 + \hat{\gamma}_p)] \\ \stackrel{(a)}{=} & \mathbb{P}\left[\eta_p > \frac{\eta_s}{\hat{\gamma}_s} - 1, \eta_s < \hat{\gamma}_s\right] \\ & + \mathbb{P}\left[\frac{\eta_s}{\hat{\gamma}_s} - 1 < \eta_p < \hat{\gamma}_p + \hat{\gamma}_s + \hat{\gamma}_p\hat{\gamma}_s - \eta_s, \hat{\gamma}_s < \eta_s < \hat{\gamma}_s(1 + \hat{\gamma}_p)\right],\end{aligned}\quad (21)$$

where (a) is obtained by first applying

$$\begin{aligned}& \mathbb{P}\left[\frac{\eta_s}{\hat{\gamma}_s} - 1 < \eta_p \leq \hat{\gamma}_p, \eta_s < \hat{\gamma}_s(1 + \hat{\gamma}_p)\right] \\ = & \mathbb{P}\left[\frac{\eta_s}{\hat{\gamma}_s} - 1 < \eta_p \leq \hat{\gamma}_p, \eta_s < \hat{\gamma}_s\right] + \mathbb{P}\left[\frac{\eta_s}{\hat{\gamma}_s} - 1 < \eta_p \leq \hat{\gamma}_p, \hat{\gamma}_s < \eta_s < \hat{\gamma}_s(1 + \hat{\gamma}_p)\right],\end{aligned}\quad (22)$$

and then combining some of the terms. Since  $\frac{\eta_s}{\hat{\gamma}_s} - 1 < 0$  if  $\eta_s < \hat{\gamma}_s$ , it means the constraint  $\eta_p > \frac{\eta_s}{\hat{\gamma}_s} - 1$  in the first term of (21) can always be satisfied. Finally,  $\mathcal{P}^{\text{CPA}}$  can be denoted as

$$\begin{aligned}\mathcal{P}^{\text{CPA}} = & \mathbb{P}[\eta_s < \hat{\gamma}_s] \\ & + \mathbb{P}\left[\frac{\eta_s}{\hat{\gamma}_s} - 1 < \eta_p < \hat{\gamma}_p + \hat{\gamma}_s + \hat{\gamma}_p\hat{\gamma}_s - \eta_s, \hat{\gamma}_s < \eta_s < \hat{\gamma}_s(1 + \hat{\gamma}_p)\right] \\ = & \mathbb{P}[|h_s|^2 < \hat{\tau}_s] \\ & + \mathbb{P}\left[\frac{|h_s|^2}{\hat{\gamma}_s} - \frac{1}{\rho_m} < |h_p|^2 < \hat{\tau}_p + \hat{\tau}_s + \hat{\tau}_p\hat{\gamma}_s - |h_s|^2, \hat{\tau}_s < |h_s|^2 < \hat{\tau}_s(1 + \hat{\gamma}_p)\right],\end{aligned}\quad (23)$$

where  $\hat{\tau}_s = \frac{\hat{\gamma}_s}{\rho_s}$  and  $\hat{\tau}_p = \frac{\hat{\gamma}_p}{\rho_p}$ . In the following, the outage performance of the two scheduling schemes with CPA strategy will be analyzed based on (23).

### B. Outage Performance Analysis of the GUS Scheme with CPA Strategy

According to (1),  $U_1$  and  $U_2$  will be scheduled in GUS scheme. For space limitations, we only consider the case regarding  $U_1$  as the primary user in this paper, and the case regarding  $U_2$  as the primary user can be derived similarly. Hence, in the following, we focus on investigating the outage performance of  $U_2$ , whose outage probability is given in the following theorem.

*Theorem 1:* For GUS scheme with CPA strategy, the outage probability of the secondary user  $U_2$  can be approximated as the following 3 cases.

Case 1: if  $\hat{\gamma}_s \geq 1$ ,

$$\begin{aligned} \mathcal{P}_{\text{GUS}}^{\text{CPA}} \approx & K \left( - \sum_{l_1=0}^L \Psi_{l_1} e^{-\mu_{l_1} \hat{\tau}_s} \right)^{K-1} - (K-1) \left( - \sum_{l_1=0}^L \Psi_{l_1} e^{-\mu_{l_1} \hat{\tau}_s} \right)^K \\ & + K(K-1) \Xi_{K-2} e^{-\mu_{l_1} (\hat{\tau}_s + \hat{\tau}_p + \hat{\tau}_p \hat{\gamma}_s)} \nu(\Delta_1; \hat{\tau}_s, m_{i1}) \\ & + K(K-1) \Xi_{K-2} \frac{1}{\Delta_2} (e^{-\Delta_2 m_{i1}} - e^{-\Delta_2 \hat{\tau}_s}). \end{aligned} \quad (24)$$

Case 2: if  $\hat{\gamma}_s < 1$  and  $\hat{\gamma}_p > \frac{\hat{\gamma}_s}{1-\hat{\gamma}_s}$ ,

$$\begin{aligned} \mathcal{P}_{\text{GUS}}^{\text{CPA}} \approx & K \left( - \sum_{l_1=0}^L \Psi_{l_1} e^{-\mu_{l_1} \hat{\tau}_s} \right)^{K-1} - (K-1) \left( - \sum_{l_1=0}^L \Psi_{l_1} e^{-\mu_{l_1} \hat{\tau}_s} \right)^K \\ & + K(K-1) \Xi_{K-2} e^{-\mu_{l_1} (\hat{\tau}_s + \hat{\tau}_p + \hat{\tau}_p \hat{\gamma}_s)} (\nu(\Delta_1; \hat{\tau}_s, m_{i2}) + \nu(\Delta_1; \frac{\hat{\tau}_s}{1-\hat{\gamma}_s}, \hat{\tau}_s(1+\hat{\gamma}_p))) \\ & + K(K-1) \Xi_{K-2} \left( \frac{e^{-\Delta_2 m_{i2}} - e^{-\Delta_2 \hat{\tau}_s}}{\Delta_2} + e^{\frac{\mu_{l_1}}{\rho_m}} \frac{e^{-\Delta_3 \hat{\tau}_s(1+\hat{\gamma}_p)} - e^{-\Delta_3 \frac{\hat{\tau}_s}{1-\hat{\gamma}_s}}}{\Delta_3} \right). \end{aligned} \quad (25)$$

Case 3: if  $\hat{\gamma}_s < 1$  and  $\hat{\gamma}_p \leq \frac{\hat{\gamma}_s}{1-\hat{\gamma}_s}$ ,

$$\begin{aligned} \mathcal{P}_{\text{GUS}}^{\text{CPA}} \approx & K \left( - \sum_{l_1=0}^L \Psi_{l_1} e^{-\mu_{l_1} \hat{\tau}_s} \right)^{K-1} - (K-1) \left( - \sum_{l_1=0}^L \Psi_{l_1} e^{-\mu_{l_1} \hat{\tau}_s} \right)^K \\ & + K(K-1) \Xi_{K-2} e^{-\mu_{l_1} (\hat{\tau}_s + \hat{\tau}_p + \hat{\tau}_p \hat{\gamma}_s)} \nu(\Delta_1; \hat{\tau}_s, m_{i2}) \\ & + K(K-1) \Xi_{K-2} \frac{e^{-\Delta_2 m_{i2}} - e^{-\Delta_2 \hat{\tau}_s}}{\Delta_2}. \end{aligned} \quad (26)$$

Where,  $m_{i1} = \min\{\hat{\tau}_s + \hat{\tau}_s \hat{\gamma}_p, \frac{1}{2}(\hat{\tau}_s + \hat{\tau}_p + \hat{\tau}_p \hat{\gamma}_s)\}$ ,  $m_{i2} = \min\{m_{i1}, \frac{\hat{\tau}_s}{1-\hat{\gamma}_s}\}$ ,  $\Delta_1 = \mu_{l_1} - \mu_{l_2} - \sum_{l=0}^L p_l \mu_l$ ,  $\Xi_{K-2} = \sum_{l_1=0}^L \Psi_{l_1} \sum_{l_2=1}^L \Psi_{l_2} \mu_{l_2} (-1)^{K-1} \sum_{\sum_{l=0}^L p_l = K-2} \binom{K-2}{p_0, \dots, p_L} \left( \prod_{l=0}^L \Psi_l^{p_l} \right)$ ,  $\Delta_2 = \mu_{l_1} + \mu_{l_2} + \sum_{l=0}^L p_l \mu_l$ ,  $\Delta_3 = \frac{1}{\hat{\gamma}_s} \mu_{l_1} + \mu_{l_2} + \sum_{l=0}^L p_l \mu_l$ , and

$$\nu(\Delta; a, b) = \begin{cases} \frac{1}{\Delta} (e^{\Delta a} - e^{\Delta b}), & \text{if } \Delta \neq 0 \\ b - a, & \text{otherwise} \end{cases}. \quad (27)$$

*Proof:* Since the relationship of the scheduled users' channel gains is determined, substituting  $|h_s|^2 \leq |h_p|^2$  into (23), the outage probability of  $U_2$  can be expressed as

$$\mathcal{P}_{\text{GUS}}^{\text{CPA}} = \mathbb{P} [|h_s|^2 < \hat{\tau}_s] + \mathbb{P} [\max\{|h_s|^2, \frac{|h_s|^2}{\hat{\gamma}_s} - \frac{1}{\rho_m}\} < |h_p|^2 < \hat{\tau}_p + \hat{\tau}_s + \hat{\tau}_p \hat{\gamma}_s - |h_s|^2], \quad (28)$$

$$\hat{\tau}_s < |h_s|^2 < \hat{\tau}_s(1 + \hat{\gamma}_p).$$

After some manipulations, we can find that in the case  $\hat{\gamma}_s \geq 1$ ,  $|h_s|^2$  is always larger than  $\frac{|h_s|^2}{\hat{\gamma}_s} - \frac{1}{\rho_m}$ . And in the case  $\hat{\gamma}_s < 1$ ,  $|h_s|^2 > \frac{|h_s|^2}{\hat{\gamma}_s} - \frac{1}{\rho_m}$  holds if  $|h_s|^2 < \frac{\hat{\tau}_s}{1 - \hat{\gamma}_s}$ ; and  $|h_s|^2 < \frac{|h_s|^2}{\hat{\gamma}_s} - \frac{1}{\rho_m}$  holds if  $|h_s|^2 > \frac{\hat{\tau}_s}{1 - \hat{\gamma}_s}$ .

Therefore,  $\mathcal{P}_{\text{GUS}}^{\text{CPA}}$  can be converted to the following two cases. Case 1, if  $\hat{\gamma}_s \geq 1$ ,

$$\mathcal{P}_{\text{GUS}}^{\text{CPA}} = \mathbb{P} [|h_s|^2 < \hat{\tau}_s] + \mathbb{P} [|h_s|^2 < |h_p|^2 < \hat{\tau}_p + \hat{\tau}_s + \hat{\tau}_p \hat{\gamma}_s - |h_s|^2, \hat{\tau}_s < |h_s|^2 < m_{i1}], \quad (29)$$

where  $m_{i1} = \min\{\hat{\tau}_s + \hat{\tau}_s \hat{\gamma}_p, \frac{1}{2}(\hat{\tau}_s + \hat{\tau}_p + \hat{\tau}_p \hat{\gamma}_s)\}$  and the constraint  $|h_s|^2 < \frac{1}{2}(\hat{\tau}_s + \hat{\tau}_p + \hat{\tau}_p \hat{\gamma}_s)$  is obtained from  $|h_s|^2 < \hat{\tau}_p + \hat{\tau}_s + \hat{\tau}_p \hat{\gamma}_s - |h_s|^2$ . Substituting the joint PDF in (8) into (29), we have

$$\begin{aligned} \mathcal{P}_{\text{GUS}}^{\text{CPA}} &= F_{|h_{K-1}|^2}(\hat{\tau}_s) \\ &+ K(K-1) \int_{\hat{\tau}_s}^{m_{i1}} [F_{|h|^2}(\hat{\tau}_s + \hat{\tau}_p + \hat{\tau}_p \hat{\gamma}_s - x) - F_{|h|^2}(x)] f_{|h|^2}(x) F_{|h|^2}(x)^{K-2} dx. \end{aligned} \quad (30)$$

In the following, the expression of  $F_{|h|^2}(x)^{K-2}$  is derived first. For ease of calculation, we rewrite (9) as

$$F_{|h|^2}(x) \approx - \sum_{l=0}^L \Psi_l e^{-\mu_l x}, \quad (31)$$

where  $\Psi_0 = - \sum_{l=1}^L \Psi_l$  and  $\mu_0 = 0$ . Based on (31), we can derive the following expression

$$\begin{aligned} [F_{|h|^2}(x)]^M &\approx \left( - \sum_{l=0}^L \Psi_l e^{-\mu_l x} \right)^M \\ &\approx (-1)^M \sum_{\sum_{l=0}^L p_l = M} \binom{M}{p_0, \dots, p_L} \left( \prod_{l=0}^L \Psi_l^{p_l} \right) e^{-\sum_{l=0}^L p_l \mu_l x}. \end{aligned} \quad (32)$$

Furthermore, the CDF of the second-largest order statistics is [28]

$$F_{|h_2|^2}(x) = K F_{|h|^2}(x)^{K-1} - (K-1) F_{|h|^2}(x)^K. \quad (33)$$

Substituting (33) and (32) into (30) and with some manipulations, we can obtain (24).

Case 2, if  $\hat{\gamma}_s < 1$ , we have

$$\begin{aligned} \mathcal{P}_{\text{GUS}}^{\text{CPA}} &= \mathbb{P} [|h_s|^2 < \hat{\tau}_s] + \mathbb{P} [|h_s|^2 < |h_p|^2 < \hat{\tau}_p + \hat{\tau}_s + \hat{\tau}_p \hat{\gamma}_s - |h_s|^2, \hat{\tau}_s < |h_s|^2 < m_{i2}], \\ &+ \mathbb{P} \left[ \frac{|h_s|^2}{\hat{\gamma}_s} - \frac{1}{\rho_m} < |h_p|^2 < \hat{\tau}_p + \hat{\tau}_s + \hat{\tau}_p \hat{\gamma}_s - |h_s|^2, \frac{\hat{\tau}_s}{1 - \hat{\gamma}_s} < |h_s|^2 < \hat{\tau}_s(1 + \hat{\gamma}_p) \right], \end{aligned} \quad (34)$$

where  $m_{i2} = \min\{m_{i1}, \frac{\hat{\tau}_s}{1 - \hat{\gamma}_s}\}$ .

With some manipulations, we have  $\frac{\hat{\tau}_s}{1-\hat{\gamma}_s} < \hat{\tau}_s(1+\hat{\gamma}_p)$ , if  $\hat{\gamma}_p > \frac{\hat{\gamma}_s}{1-\hat{\gamma}_s}$ . Hence, for the case  $\hat{\gamma}_s < 1$  and  $\hat{\gamma}_p > \frac{\hat{\gamma}_s}{1-\hat{\gamma}_s}$ , substituting (8) into (34), we have

$$\begin{aligned}\mathcal{P}_{\text{GUS}}^{\text{CPA}} &= F_{|h_2|^2}(\hat{\tau}_s) + K(K-1) \\ &\times \int_{\frac{\hat{\tau}_s}{1-\hat{\gamma}_s}}^{\hat{\tau}_s(1+\hat{\gamma}_p)} [F_{|h|^2}(\hat{\tau}_s + \hat{\tau}_p + \hat{\tau}_p \hat{\gamma}_s - x) - F_{|h|^2}(\frac{x}{\hat{\gamma}_s} - \frac{1}{\rho_m})] f_{|h|^2}(x) F_{|h|^2}(x)^{K-2} dx \\ &+ K(K-1) \int_{\hat{\tau}_s}^{m_{i2}} [F_{|h|^2}(\hat{\tau}_s + \hat{\tau}_p + \hat{\tau}_p \hat{\gamma}_s - x) - F_{|h|^2}(x)] f_{|h|^2}(x) F_{|h|^2}(x)^{K-2} dx.\end{aligned}\quad (35)$$

Then, following the same lines of deriving (24),  $\mathcal{P}_{\text{GUS}}^{\text{CPA}}$  can be calculated as (25). Similarly, for the case  $\hat{\gamma}_s < 1$  and  $\hat{\gamma}_p \leq \frac{\hat{\gamma}_s}{1-\hat{\gamma}_s}$ ,  $\mathcal{P}_{\text{GUS}}^{\text{CPA}}$  can be calculated as (26). The proof of Theorem 1 is completed.  $\blacksquare$

The expressions in Theorem 1 are quite complicated. To get some insights, we further derive the outage approximation expressions at the high SNR region.

*Corollary 1:* When  $\rho_m \rightarrow \infty$ , the high SNR approximation of  $\mathcal{P}_{\text{GUS}}^{\text{CPA}}$  can be expressed as the following 3 cases.

Case 1: if  $\hat{\gamma}_s \geq 1$ ,

$$\begin{aligned}\vec{\mathcal{P}}_{\text{GUS}}^{\text{CPA}} &\approx K(S_L \hat{\tau}_s)^{K-1} - (K-1)(S_L \hat{\tau}_s)^K \\ &+ K(K-1)(S_L)^K \left[ (\hat{\tau}_s + \hat{\tau}_p + \hat{\tau}_p \hat{\gamma}_s) \frac{m_{i1}^{K-1} - \hat{\tau}_s^{K-1}}{K-1} - \frac{2}{K} (m_{i1}^K - \hat{\tau}_s^K) \right].\end{aligned}\quad (36)$$

Case 2: if  $\hat{\gamma}_s < 1$  and  $\hat{\gamma}_p > \frac{\hat{\gamma}_s}{1-\hat{\gamma}_s}$ ,

$$\begin{aligned}\vec{\mathcal{P}}_{\text{GUS}}^{\text{CPA}} &= K(S_L \hat{\tau}_s)^{K-1} - (K-1)(S_L \hat{\tau}_s)^K + K(K-1)(S_L)^K \\ &\times \left[ (\hat{\tau}_s + \hat{\tau}_p + \hat{\tau}_p \hat{\gamma}_s) \frac{m_{i2}^{K-1} - \hat{\tau}_s^{K-1}}{K-1} - \frac{1+\hat{\gamma}_s}{K \hat{\gamma}_s} ((\hat{\tau}_s(1+\hat{\gamma}_p))^K - (\frac{\hat{\tau}_s}{1-\hat{\gamma}_s})^K) \right. \\ &\left. + \frac{\hat{\tau}_s + \hat{\tau}_p + \hat{\tau}_p \hat{\gamma}_s + \rho_m^{-1}}{K-1} [(\hat{\tau}_s(1+\hat{\gamma}_p))^{K-1} - (\frac{\hat{\tau}_s}{1-\hat{\gamma}_s})^{K-1}] - \frac{2}{K} (m_{i2}^K - \hat{\tau}_s^K) \right].\end{aligned}\quad (37)$$

Case 3: if  $\hat{\gamma}_s < 1$  and  $\hat{\gamma}_p \leq \frac{\hat{\gamma}_s}{1-\hat{\gamma}_s}$

$$\begin{aligned}\vec{\mathcal{P}}_{\text{GUS}}^{\text{CPA}} &= K(S_L \hat{\tau}_s)^{K-1} - (K-1)(S_L \hat{\tau}_s)^K \\ &+ K(K-1)(S_L)^K \left[ (\hat{\tau}_s + \hat{\tau}_p + \hat{\tau}_p \hat{\gamma}_s) \frac{m_{i2}^{K-1} - \hat{\tau}_s^{K-1}}{K-1} - \frac{2}{K} (m_{i2}^K - \hat{\tau}_s^K) \right].\end{aligned}\quad (38)$$

Note that,  $S_L = \sum_{l=1}^L \Psi_l \mu_l$ . The secondary user  $U_2$  can achieve a diversity order of  $K-1$  in all three cases.

*Proof:* It is quite involved to derive the high SNR approximation expressions with (24), (25), and (26). In the following, (30) and (35) are used to derive the approximation expressions. When  $\rho_m \rightarrow \infty$ , we have  $m_{i1} \rightarrow 0$ ,  $m_{i2} \rightarrow 0$ , and  $\hat{\tau}_s(1+\hat{\gamma}_p) \rightarrow 0$ .

If  $x \rightarrow 0$ , (9) and (10) can be respectively approximated as

$$F_{|h|^2}(x) \approx \sum_{l=1}^L \Psi_l \mu_l x, \quad (39)$$

and

$$f_{|h|^2}(x) \approx \sum_{l=1}^L \Psi_l \mu_l (1 - \mu_l x) = \sum_{l=1}^L \Psi_l \mu_l. \quad (40)$$

Hence, substituting (39) and (40) into (35), we have

$$\begin{aligned} \vec{\mathcal{P}}_{\text{GUS}}^{\text{CPA}} \approx & K(S_L \hat{\tau}_s)^{K-1} - (K-1)(S_L \hat{\tau}_s)^K \\ & + K(K-1) \int_{\frac{\hat{\tau}_s}{1-\hat{\gamma}_s}}^{\hat{\tau}_s(1+\hat{\gamma}_p)} S_L [(\hat{\tau}_s + \hat{\tau}_p + \hat{\tau}_p \hat{\gamma}_s - x) - (\frac{x}{\hat{\gamma}_s} - \frac{1}{\rho_m})] S_L (S_L x)^{K-2} dx \\ & + K(K-1) \int_{\hat{\tau}_s}^{m_{i2}} S_L [(\hat{\tau}_s + \hat{\tau}_p + \hat{\tau}_p \hat{\gamma}_s - x) - x] S_L (S_L x)^{K-2} dx \end{aligned} \quad (41)$$

After some algebra manipulations, we can obtain (37). Furthermore, (36) and (38) can be derived in the same way. It can be observed that the first terms of (36), (37), and (38) are proportional to  $\rho_m^{-(K-1)}$ , and other terms are proportional to  $\rho_m^{-K}$ . By applying (7), we know that the secondary user  $U_2$  can achieve a diversity order of  $K-1$ , and the proof is completed. ■

*Remark 2:* Corollary 1 shows that the target SINR of the secondary user,  $\hat{\tau}_s$ , plays an important role in the outage performance of  $U_2$ . Particularly, in the high SNR region, the outage performance of  $U_2$  is related to  $\hat{\tau}_s$  and the total number of users  $K$ , but irrelevant to the target rate of the primary user.

### C. Outage Performance Analysis of the CUS Scheme with CPA Strategy

Due to space limitations, we only consider the case regarding the user with the largest CDF value as the primary user in this paper, and the case regarding the second-largest CDF user as the primary user can be analyzed similarly.

*Theorem 2:* For CUS scheme with CPA strategy, the outage probability of the user with the second-largest CDF value can be approximated as

$$\mathcal{P}_{\text{CUS}}^{\text{CPA}} \approx K \sum_{l_1=1}^L \Psi_{l_1} (1 - e^{-\mu_{l_1} \hat{\tau}_s})^{K-1} - (K-1) \sum_{l_1=1}^L \Psi_{l_1} (1 - e^{-\mu_{l_1} \hat{\tau}_s})^K + T_1 - T_2, \quad (42)$$

where  $T_1$  and  $T_2$  are calculated with Tables I and II, respectively.  $\epsilon_1 = \frac{\hat{\tau}_s + \hat{\tau}_p + \hat{\tau}_p \hat{\gamma}_s}{R^\alpha + 2}$ ,  $\epsilon_2 = \frac{1}{2}(\hat{\tau}_s + \hat{\tau}_p + \hat{\tau}_p \hat{\gamma}_s)$ ,  $\epsilon_3 = \frac{R^\alpha + 1}{R^\alpha + 2}(\hat{\tau}_s + \hat{\tau}_p + \hat{\tau}_p \hat{\gamma}_s)$ ,  $\epsilon_4 = \frac{\hat{\tau}_s}{1 - \hat{\gamma}_s - R^\alpha \hat{\gamma}_s}$ ,  $\epsilon_5 = \frac{\hat{\tau}_s}{1 - \hat{\gamma}_s}$ ,  $\epsilon_6 = \frac{(R^\alpha + 1) \hat{\tau}_s}{R^\alpha + 1 - \hat{\gamma}_s}$ , and  $x$  represents  $\hat{\tau}_s + \hat{\tau}_p(1 + \hat{\gamma}_s) - y$  and  $\frac{1}{\hat{\gamma}_s} y - \frac{1}{\rho_m}$  in Table I and Table II, respectively.  $F_{X,Y'}^{\text{CUS},I}(x, y)$ ,  $F_{X,Y'}^{\text{CUS},II}(x, y)$ , and  $F_{X,Y'}^{\text{CUS},III}(x, y)$  denote the partial derivatives of (12), (13) and (14) with respect to  $y$ , respectively, and we omit the expressions due to space limitations.  $\mathcal{G}[a, b; F_{X,Y'}^{\text{CUS}}(x, y)]$  denotes applying

TABLE I  
CALCULATION OF  $T_1$

Assumption 1	Assumption 2	$T_1$
$\epsilon_2 > \hat{\tau}_s(1 + \hat{\gamma}_p)$	$\epsilon_1 > \hat{\tau}_s(1 + \hat{\gamma}_p)$	$\mathcal{G}[\hat{\tau}_s, \hat{\tau}_s(1 + \hat{\gamma}_p); F_{X,Y'}^{\text{CUS},\text{I}}(x, y)]$
	$\hat{\tau}_s < \epsilon_1 < \hat{\tau}_s(1 + \hat{\gamma}_p)$	$\mathcal{G}[\hat{\tau}_s, \epsilon_1; F_{X,Y'}^{\text{CUS},\text{I}}(x, y)] + \mathcal{G}[\epsilon_1, \hat{\tau}_s(1 + \hat{\gamma}_p); F_{X,Y'}^{\text{CUS},\text{II}}(x, y)]$
	$\epsilon_1 < \hat{\tau}_s$	$\mathcal{G}[\hat{\tau}_s, \hat{\tau}_s(1 + \hat{\gamma}_p); F_{X,Y'}^{\text{CUS},\text{II}}(x, y)]$
$\hat{\tau}_s < \epsilon_2 < \hat{\tau}_s(1 + \hat{\gamma}_p)$	$\epsilon_1 < \hat{\tau}_s \text{ and } \epsilon_3 < \hat{\tau}_s(1 + \hat{\gamma}_p)$	$\mathcal{G}[\hat{\tau}_s, \epsilon_2; F_{X,Y'}^{\text{CUS},\text{II}}(x, y)] + \mathcal{G}[\epsilon_2, \epsilon_3; F_{X,Y'}^{\text{CUS},\text{III}}(x, y)]$
	$\epsilon_1 < \hat{\tau}_s \text{ and } \epsilon_3 > \hat{\tau}_s(1 + \hat{\gamma}_p)$	$\mathcal{G}[\hat{\tau}_s, \epsilon_2; F_{X,Y'}^{\text{CUS},\text{II}}(x, y)] + \mathcal{G}[\epsilon_2, \hat{\tau}_s(1 + \hat{\gamma}_p); F_{X,Y'}^{\text{CUS},\text{III}}(x, y)]$
	$\hat{\tau}_s < \epsilon_1 < \epsilon_2 \text{ and } \epsilon_3 < \hat{\tau}_s(1 + \hat{\gamma}_p)$	$\mathcal{G}[\hat{\tau}_s, \epsilon_1; F_{X,Y'}^{\text{CUS},\text{I}}(x, y)] + \mathcal{G}[\epsilon_1, \epsilon_2; F_{X,Y'}^{\text{CUS},\text{II}}(x, y)] + \mathcal{G}[\epsilon_2, \epsilon_3; F_{X,Y'}^{\text{CUS},\text{III}}(x, y)]$
	$\hat{\tau}_s < \epsilon_1 < \epsilon_2 \text{ and } \epsilon_3 > \hat{\tau}_s(1 + \hat{\gamma}_p)$	$\mathcal{G}[\hat{\tau}_s, \epsilon_1; F_{X,Y'}^{\text{CUS},\text{I}}(x, y)] + \mathcal{G}[\epsilon_1, \epsilon_2; F_{X,Y'}^{\text{CUS},\text{II}}(x, y)] + \mathcal{G}[\epsilon_2, \hat{\tau}_s(1 + \hat{\gamma}_p); F_{X,Y'}^{\text{CUS},\text{III}}(x, y)]$
$\epsilon_2 < \hat{\tau}_s$	$\epsilon_3 < \hat{\tau}_s$	0
	$\hat{\tau}_s < \epsilon_3 < \hat{\tau}_s(1 + \hat{\gamma}_p)$	$\mathcal{G}[\hat{\tau}_s, \epsilon_3; F_{X,Y'}^{\text{CUS},\text{III}}(x, y)]$
	$\epsilon_3 > \hat{\tau}_s(1 + \hat{\gamma}_p)$	$\mathcal{G}[\hat{\tau}_s, \hat{\tau}_s(1 + \hat{\gamma}_p); F_{X,Y'}^{\text{CUS},\text{III}}(x, y)]$

TABLE II  
CALCULATION OF  $T_2$

Assumption 1	Assumption 2	Assumption 3	$T_2$
$\hat{\gamma}_s > 1$	$R^\alpha + 1 < \hat{\gamma}_s$	—	0
	$R^\alpha + 1 > \hat{\gamma}_s$	$\epsilon_6 > \hat{\tau}_s(1 + \hat{\gamma}_p)$	0
		$\epsilon_6 < \hat{\tau}_s(1 + \hat{\gamma}_p)$	$\mathcal{G}[\epsilon_6, \hat{\tau}_s(1 + \hat{\gamma}_p); F_{X,Y'}^{\text{CUS},\text{III}}(x, y)]$
$\hat{\gamma}_s < 1$	$\hat{\gamma}_s < \frac{\hat{\gamma}_p}{1 + \hat{\gamma}_p}$	$\hat{\gamma}_s > \frac{1}{(R^\alpha + 1)(\hat{\gamma}_p + 1)}$	$\mathcal{G}[\epsilon_6, \epsilon_5; F_{X,Y'}^{\text{CUS},\text{III}}(x, y)] + \mathcal{G}[\epsilon_5, \hat{\tau}_s(1 + \hat{\gamma}_p); F_{X,Y'}^{\text{CUS},\text{II}}(x, y)]$
		$\hat{\gamma}_s < \frac{1}{(R^\alpha + 1)(\hat{\gamma}_p + 1)}$	$\mathcal{G}[\epsilon_6, \epsilon_5; F_{X,Y'}^{\text{CUS},\text{III}}(x, y)] + \mathcal{G}[\epsilon_5, \epsilon_4; F_{X,Y'}^{\text{CUS},\text{II}}(x, y)] + \mathcal{G}[\epsilon_4, \hat{\tau}_s(1 + \hat{\gamma}_p); F_{X,Y'}^{\text{CUS},\text{I}}(x, y)]$
	$\hat{\gamma}_s > \frac{\hat{\gamma}_p}{1 + \hat{\gamma}_p}$	$\hat{\gamma}_s > \frac{(R^\alpha + 1)\hat{\gamma}_p}{1 + \hat{\gamma}_p}$	$\mathcal{G}[\epsilon_6, \hat{\tau}_s(1 + \hat{\gamma}_p); F_{X,Y'}^{\text{CUS},\text{III}}(x, y)]$
		$\hat{\gamma}_s < \frac{(R^\alpha + 1)\hat{\gamma}_p}{1 + \hat{\gamma}_p}$	0

Gaussian-Chebyshev quadrature [33] to the integral of  $F_{X,Y'}^{\text{CUS}}(x, y)$  with integral interval  $(a, b)$ , namely,  $\mathcal{G}[a, b; F_{X,Y'}^{\text{CUS}}(x, y)] \approx \int_a^b F_{X,Y'}^{\text{CUS}}(x, y) dy$ .

*Proof:* Please refer to Appendix B. ■

*Corollary 2:* In CUS scheme with CPA strategy, the user with the second-largest CDF value can achieve a diversity order  $K - 1$ .

*Proof:* It can be observed from the proof of Theorem 2 that, it is quite involved to derive the achieved diversity order by first deriving the high SNR approximation of the outage probability expressions. As an alternative, in the following, the upper bound of the outage probability will be derived first and then be applied to derive the achieved diversity order. We can derive from (23) that

$$\begin{aligned}\mathcal{P}^{\text{CPA}} &\leq \mathbb{P} [|h_s|^2 < \hat{\tau}_s] + \mathbb{P} [\hat{\tau}_s < |h_s|^2 < \hat{\tau}_s(1 + \hat{\gamma}_p)] \\ &= \mathbb{P} [|h_s|^2 < \hat{\tau}_s(1 + \hat{\gamma}_p)].\end{aligned}\quad (43)$$

Then, applying (16), the upper bound of the secondary user in CDF-based scheduling can be expressed as

$$\mathcal{P}^{\text{CPA}} \leq K \sum_{l_1=1}^L \Psi_{l_1} (1 - e^{-\mu_{l_1} \hat{\tau}_s(1 + \hat{\gamma}_p)})^{K-1} - (K-1) \sum_{l_1=1}^L \Psi_{l_1} (1 - e^{-\mu_{l_1} \hat{\tau}_s(1 + \hat{\gamma}_p)})^K. \quad (44)$$

When the transmit SNR  $\rho_m \rightarrow \infty$ , by using  $1 - e^{-x} \approx x$ , we have

$$\mathcal{P}^{\text{CPA}} \leq K \sum_{l_1=1}^L \Psi_{l_1} (\mu_{l_1} \hat{\tau}_s (1 + \hat{\gamma}_p))^{K-1} - (K-1) \sum_{l_1=1}^L \Psi_{l_1} (\mu_{l_1} \hat{\tau}_s (1 + \hat{\gamma}_p))^K. \quad (45)$$

By applying the definition of diversity order, we know that the secondary user can achieve a diversity order of  $K-1$ , and the proof is completed. ■

In CPA strategy, the primary user,  $U_p$ , can achieve the same performance as it solely occupies the channel. By applying the results in [25], [32], it can be easily demonstrated that a diversity order of  $K$  is achievable for  $U_p$  in both GUS and CUS schemes. Meanwhile, Corollaries 1 and 2 illustrate that the secondary users in both GUS and CUS schemes can achieve the diversity orders of  $K-1$ . Hence, it can be concluded that full diversity orders can be achieved for CPA strategy in both GUS and CUS schemes.

The CUS scheme not only can provide a fair access opportunity for all the users, but Corollary 2 illustrates that it can also achieve full diversity order as GUS scheme for CPA strategy. It is known that random user scheduling can also provide a fair access opportunity for the users, but it can not effectively employ multi-user diversity. Hence the CUS scheme will achieve much better outage performance than the random user selection scheme, especially for the system with many users, which will be shown in the simulation results.

*Remark 3:* Compared with NOMA transmission in [25], [32], an interesting phenomenon can be observed from RSMA transmission in the application of CPA strategy. Specifically, in NOMA transmission, the achieved diversity order of the secondary user is restricted by the channel quality of the primary user [25], [32], however, such restriction vanishes in RSMA transmission. For example, in GUS scheme, assuming  $U_2$  is the primary user, it can be demonstrated that the

achieved diversity order of the secondary user,  $U_1$ , is also  $K$  by applying (43). However, in NOMA transmission [25], [32],  $U_1$  in GUS scheme can only achieve a diversity order of  $K - 1$ . In other words, in RSMA transmission, the secondary user's achieved diversity order with CPA strategy is only determined by its own channel quality.

## V. OUTAGE PERFORMANCE ANALYSIS OF THE FPA STRATEGY

In this section, we first derive the outage probability expression of FPA strategy. Then, we analyze the outage performance of each scheduling scheme with FPA strategy.

### A. Outage Probability of the FPA Strategy

According to Section III-B2, the outage probability of  $U_i$  with FPA strategy can be expressed as

$$\begin{aligned} \mathcal{P}_i^{\text{FPA}} = & \mathbb{P} \left[ \eta_j < \eta_i < \eta_j + \eta_j^2, \frac{1}{2} \log_2(1 + \eta_i + \eta_j) < \hat{R}_i \right] \\ & + \mathbb{P} \left[ \eta_j + \eta_j^2 < \eta_i, \log_2(1 + \frac{\eta_i}{\eta_j + 1}) < \hat{R}_i \right] \\ & + \mathbb{P} \left[ \eta_i < \eta_j < \eta_i + \eta_i^2, \frac{1}{2} \log_2(1 + \eta_i + \eta_j) < \hat{R}_i \right] \\ & + \mathbb{P} \left[ \eta_i + \eta_i^2 < \eta_j, \log_2(1 + \eta_i) < \hat{R}_i \right], \end{aligned} \quad (46)$$

where  $\hat{R}_i$  denotes the target data rate of  $U_i$ . It should be noted that  $2^{2\hat{R}_i} - 1 = \hat{\gamma}_i^2 + 2\hat{\gamma}_i$ , and  $\hat{\gamma}_i = 2^{\hat{R}_i} - 1$  represents the target SINR of  $U_i$ . After some manipulations, (46) can be converted to

$$\begin{aligned} \mathcal{P}_i^{\text{FPA}} = & \mathbb{P} \left[ \eta_j < \eta_i < \eta_j + \eta_j^2, \eta_j < \hat{\gamma}_i \right] + \mathbb{P} \left[ \eta_j < \eta_i < \hat{\gamma}_i^2 + 2\hat{\gamma}_i - \eta_j, \hat{\gamma}_i < \eta_j < \hat{\gamma}_i + \frac{1}{2}\hat{\gamma}_i^2 \right] \\ & + \mathbb{P} \left[ \eta_j + \eta_j^2 < \eta_i < \hat{\gamma}_i(\eta_j + 1), \eta_j < \hat{\gamma}_i \right] \\ & + \mathbb{P} \left[ \eta_i < \eta_j < \eta_i + \eta_i^2, \eta_i < \hat{\gamma}_i \right] + \mathbb{P} \left[ \eta_i < \eta_j < \hat{\gamma}_i^2 + 2\hat{\gamma}_i - \eta_i, \hat{\gamma}_i < \eta_i < \hat{\gamma}_i + \frac{1}{2}\hat{\gamma}_i^2 \right] \\ & + \mathbb{P} \left[ \eta_i + \eta_i^2 < \eta_j, \eta_i < \hat{\gamma}_i \right]. \end{aligned} \quad (47)$$

By combining some of the terms in (47), we have

$$\begin{aligned} \mathcal{P}_i^{\text{FPA}} = & \mathbb{P} \left[ \eta_j < \eta_i < \hat{\gamma}_i(\eta_j + 1), \eta_j < \hat{\gamma}_i \right] + \mathbb{P} \left[ \eta_j < \eta_i < \hat{\gamma}_i^2 + 2\hat{\gamma}_i - \eta_j, \hat{\gamma}_i < \eta_j < \hat{\gamma}_i + \frac{1}{2}\hat{\gamma}_i^2 \right] \\ & + \mathbb{P} \left[ \eta_i < \eta_j, \eta_i < \hat{\gamma}_i \right] + \mathbb{P} \left[ \eta_i < \eta_j < \hat{\gamma}_i^2 + 2\hat{\gamma}_i - \eta_i, \hat{\gamma}_i < \eta_i < \hat{\gamma}_i + \frac{1}{2}\hat{\gamma}_i^2 \right]. \end{aligned} \quad (48)$$

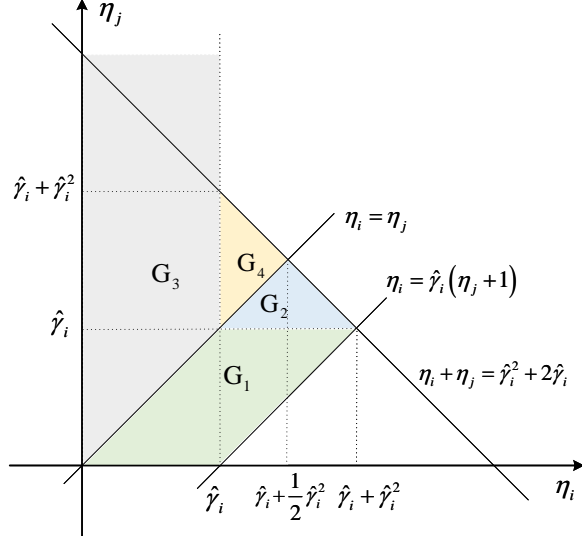


Fig. 2. The integral regions of (48), where  $G_1$ ,  $G_2$ ,  $G_3$ , and  $G_4$  correspond to the integral regions of the first, second, third, and fourth terms of (48), respectively.

To further simplify the calculation complexity, we draw the integral regions of (48) in Fig. 2.

It can be observed from Fig. 2 that  $\mathcal{P}_i^{\text{FPA}}$  can be finally expressed as

$$\begin{aligned} \mathcal{P}_i^{\text{FPA}} &= \mathbb{P} \left[ \hat{\gamma}_i < \eta_i < \hat{\gamma}_i^2 + \hat{\gamma}_i, \frac{1}{\hat{\gamma}_i} \eta_i - 1 < \eta_j < \hat{\gamma}_i^2 + 2\hat{\gamma}_i - \eta_i \right] + \mathbb{P} [\eta_i < \hat{\gamma}_i] \\ &= \mathbb{P} \left[ \hat{\tau}_i < |h_i|^2 < \hat{\gamma}_i \hat{\tau}_i + \hat{\tau}_i, \frac{1}{\hat{\gamma}_i} |h_i|^2 - \frac{1}{\rho_m} < |h_j|^2 < \hat{\tau}_i \hat{\gamma}_i + 2\hat{\tau}_i - |h_i|^2 \right] + \mathbb{P} [|h_i|^2 < \hat{\tau}_i]. \end{aligned} \quad (49)$$

Similarly, the outage probability of  $U_j$  can be expressed as

$$\begin{aligned} \mathcal{P}_j^{\text{FPA}} &= \mathbb{P} \left[ \eta_j < \eta_i < \eta_j + \eta_j^2, \frac{1}{2} \log_2(1 + \eta_i + \eta_j) < \hat{R}_j \right] \\ &\quad + \mathbb{P} \left[ \eta_j + \eta_j^2 < \eta_i, \log_2(1 + \eta_j) < \hat{R}_j \right] \\ &\quad + \mathbb{P} \left[ \eta_i < \eta_j < \eta_i + \eta_i^2, \frac{1}{2} \log_2(1 + \eta_i + \eta_j) < \hat{R}_j \right] \\ &\quad + \mathbb{P} \left[ \eta_i + \eta_i^2 < \eta_j, \log_2(1 + \frac{\eta_j}{1 + \eta_i}) < \hat{R}_j \right]. \end{aligned} \quad (50)$$

By applying the same steps of deriving (49),  $\mathcal{P}_j^{\text{FPA}}$  can be finally denoted as

$$\mathcal{P}_j^{\text{FPA}} = \mathbb{P} \left[ \hat{\tau}_j < |h_j|^2 < \hat{\gamma}_j \hat{\tau}_j + \hat{\tau}_j, \frac{1}{\hat{\gamma}_j} |h_j|^2 - \frac{1}{\rho_m} < |h_i|^2 < \hat{\tau}_j \hat{\gamma}_j + 2\hat{\tau}_j - |h_j|^2 \right] + \mathbb{P} [|h_j|^2 < \hat{\tau}_j], \quad (51)$$

where  $\hat{R}_j$  and  $\hat{\gamma}_j = 2^{\hat{R}_j} - 1$  denote the target data rate and target SINR of  $U_j$ , respectively.

## B. Outage Performance Analysis of the GUS Scheme with FPA Strategy

In the GUS scheme,  $U_1$  and  $U_2$  are scheduled and their channel gains are ordered as  $|h_1|^2 \geq |h_2|^2$ . The following theorem shows the two users' outage probabilities.

*Theorem 3:* For GUS scheme with FPA strategy, the scheduled two users' outage probabilities can be expressed as

$$\begin{aligned} \mathcal{P}_{\text{GUS},1}^{\text{FPA}} \approx & K \Xi_{K-1,l} \sum_{n=1}^L \Psi_n \mu_n (e^{-(\hat{\gamma}_1 \hat{\tau}_1 + 2\hat{\tau}_1) \sum_{l=0}^L p_l \mu_l} \nu(\chi_3; \hat{\tau}_1 + \frac{1}{2}\hat{\tau}_1 \hat{\gamma}_1, \hat{\tau}_1 + \hat{\tau}_1 \hat{\gamma}_1)) \\ & + \frac{1}{\chi_4} e^{\frac{1}{\rho_m} \sum_{l=0}^L p_l \mu_l} (e^{-\chi_4(\hat{\tau}_1 + \hat{\tau}_1 \hat{\gamma}_1)} - e^{-\chi_4 \hat{\tau}_1}) \\ & + \frac{1}{\chi_5} (e^{-\chi_5 \hat{\tau}_1} - e^{-\chi_5(\hat{\tau}_1 + \frac{1}{2}\hat{\tau}_1 \hat{\gamma}_1)}) + \left( - \sum_{l=0}^L \Psi_l e^{-\mu_l \hat{\tau}_1} \right)^K \end{aligned} \quad (52)$$

and

$$\begin{aligned} \mathcal{P}_{\text{GUS},2}^{\text{FPA}} \approx & K(K-1) \Xi_{K-2} (e^{-\mu_1(\hat{\gamma}_2 \hat{\tau}_2 + 2\hat{\tau}_2)} \nu(\Delta_1; \hat{\tau}_2, \hat{\tau}_2 + \frac{1}{2}\hat{\tau}_2 \hat{\gamma}_2) + \frac{e^{-\Delta_2(\hat{\tau}_2 + \frac{1}{2}\hat{\tau}_2 \hat{\gamma}_2)} - e^{-\Delta_2 \hat{\tau}_2}}{\Delta_2}) \\ & + K \left( - \sum_{l=0}^L \Psi_l e^{-\mu_l \hat{\tau}_2} \right)^{K-1} - (K-1) \left( - \sum_{l=0}^L \Psi_l e^{-\mu_l \hat{\tau}_2} \right)^K, \end{aligned} \quad (53)$$

respectively, where  $\chi_3 = \sum_{l=0}^L p_l \mu_l - \mu_n$ ,  $\chi_4 = \frac{1}{\hat{\gamma}_1} \sum_{l=0}^L p_l \mu_l + \mu_n$ ,  $\chi_5 = \sum_{l=0}^L p_l \mu_l + \mu_n$ .

*Proof:* Substituting  $|h_1|^2 \geq |h_2|^2$  into (49), the outage probability of  $U_1$  can be expressed as

$$\begin{aligned} \mathcal{P}_{\text{GUS},1}^{\text{FPA}} = & \mathbb{P} \left[ \hat{\tau}_1 < |h_1|^2 < \hat{\gamma}_1 \hat{\tau}_1 + \hat{\tau}_1, \frac{1}{\hat{\gamma}_1} |h_1|^2 - \frac{1}{\rho_m} < |h_2|^2 < \min\{|h_1|^2, \hat{\tau}_1 \hat{\gamma}_1 + 2\hat{\tau}_1 - |h_1|^2\} \right] \\ & + \mathbb{P} [|h_1|^2 < \hat{\tau}_1]. \end{aligned} \quad (54)$$

To simplify (54), we should compare the values of  $|h_1|^2$  and  $\hat{\tau}_1 \hat{\gamma}_1 + 2\hat{\tau}_1 - |h_1|^2$  first. It can be derived that,  $|h_1|^2 > \hat{\tau}_1 \hat{\gamma}_1 + 2\hat{\tau}_1 - |h_1|^2$  holds if  $|h_1|^2 > \hat{\tau}_1 + \frac{1}{2}\hat{\gamma}_1 \hat{\tau}_1$ , and vice versa. Note that, the condition for  $\frac{1}{\hat{\gamma}_1} |h_1|^2 - \frac{1}{\rho_m} < |h_1|^2$  in (54) is

$$\begin{cases} |h_1|^2 < \frac{\hat{\tau}_1}{1-\hat{\gamma}_1}, & \text{if } \hat{\gamma}_1 < 1 \\ \text{No constraints,} & \text{otherwise} \end{cases}. \quad (55)$$

However, in the case  $\hat{\gamma}_1 < 1$ , we have  $\hat{\gamma}_1 \hat{\tau}_1 + \hat{\tau}_1 < \frac{\hat{\tau}_1}{1-\hat{\gamma}_1}$ . Thus, based on (55), we know that, no matter  $\hat{\gamma}_1 \geq 1$  or  $\hat{\gamma}_1 < 1$ ,  $\frac{1}{\hat{\gamma}_1} |h_1|^2 - \frac{1}{\rho_m} < |h_1|^2$  always holds for  $\hat{\tau}_1 < |h_1|^2 < \hat{\gamma}_1 \hat{\tau}_1 + \hat{\tau}_1$ .

Hence,  $\mathcal{P}_{\text{GUS},1}^{\text{FPA}}$  can be further denoted as

$$\begin{aligned} \mathcal{P}_{\text{GUS},1}^{\text{FPA}} = & \mathbb{P} \left[ \hat{\tau}_1 + \frac{1}{2}\hat{\gamma}_1 \hat{\tau}_1 < |h_1|^2 < \hat{\tau}_1 + \hat{\gamma}_1 \hat{\tau}_1, \frac{1}{\hat{\gamma}_1} |h_1|^2 - \frac{1}{\rho_m} < |h_2|^2 < \hat{\tau}_1 \hat{\gamma}_1 + 2\hat{\tau}_1 - |h_1|^2 \right] \\ & + \mathbb{P} \left[ \hat{\tau}_1 < |h_1|^2 < \hat{\tau}_1 + \frac{1}{2}\hat{\gamma}_1 \hat{\tau}_1, \frac{1}{\hat{\gamma}_1} |h_1|^2 - \frac{1}{\rho_m} < |h_2|^2 < |h_1|^2 \right] \\ & + \mathbb{P} [|h_1|^2 < \hat{\tau}_1]. \end{aligned} \quad (56)$$

By applying (8), the outage probability of  $U_1$  can be expressed as

$$\begin{aligned}\mathcal{P}_{\text{GUS},1}^{\text{FPA}} = & K \int_{\hat{\tau}_1 + \frac{1}{2}\hat{\tau}_1\hat{\gamma}_1}^{\hat{\tau}_1 + \hat{\tau}_1\hat{\gamma}_1} [F_{|h|^2}(\hat{\gamma}_1\hat{\tau}_1 + 2\hat{\tau}_1 - y)^{K-1} - F_{|h|^2}(\frac{1}{\hat{\gamma}_1}y - \frac{1}{\rho_m})^{K-1}] f_{|h|^2}(y) dy \\ & + K \int_{\hat{\tau}_1}^{\hat{\tau}_1 + \frac{1}{2}\hat{\tau}_1\hat{\gamma}_1} [F_{|h|^2}(y)^{K-1} - F_{|h|^2}(\frac{1}{\hat{\gamma}_1}y - \frac{1}{\rho_m})^{K-1}] f_{|h|^2}(y) dy + F_{|h|^2}(\hat{\tau}_1)^K,\end{aligned}\quad (57)$$

where the CDF of the largest order statistics  $F_{|h_1|^2}(x) = F_{|h|^2}(x)^K$  [28] is applied. Substituting (32) and (33) into (57), and after some manipulations, we can obtain (52).

The outage probability for  $U_2$  can be derived by substituting  $|h_1|^2 \geq |h_2|^2$  into (51), namely,

$$\begin{aligned}\mathcal{P}_{\text{GUS},2}^{\text{FPA}} = & \mathbb{P} \left[ \hat{\tau}_2 < |h_2|^2 < \hat{\gamma}_2\hat{\tau}_2 + \hat{\tau}_2, \max\{|h_2|^2, \frac{1}{\hat{\gamma}_2}|h_2|^2 - \frac{1}{\rho_m}\} < |h_1|^2 < \hat{\gamma}_2\hat{\tau}_2 + 2\hat{\tau}_2 - |h_2|^2 \right] \\ & + \mathbb{P} [|h_2|^2 < \hat{\tau}_2].\end{aligned}\quad (58)$$

Note that, when  $\hat{\tau}_2 < |h_2|^2 < \hat{\gamma}_2\hat{\tau}_2 + \hat{\tau}_2$ ,  $|h_2|^2$  is always larger than  $\frac{1}{\hat{\gamma}_2}|h_2|^2 - \frac{1}{\rho_m}$ . Thus (58) can be converted to

$$\mathcal{P}_{\text{GUS},2}^{\text{FPA}} = \mathbb{P} \left[ \hat{\tau}_2 < |h_2|^2 < \hat{\gamma}_2\hat{\tau}_2 + \hat{\tau}_2, |h_2|^2 < |h_1|^2 < \hat{\gamma}_2\hat{\tau}_2 + 2\hat{\tau}_2 - |h_2|^2 \right] + \mathbb{P} [|h_2|^2 < \hat{\tau}_2]. \quad (59)$$

The constraint of  $|h_2|^2 < \hat{\gamma}_2\hat{\tau}_2 + 2\hat{\tau}_2 - |h_2|^2$  in (59) requires  $|h_2|^2 < \hat{\tau}_2 + \frac{1}{2}\hat{\gamma}_2\hat{\tau}_2$ . Thus  $\mathcal{P}_{\text{GUS},2}^{\text{FPA}}$  can be finally denoted as

$$\mathcal{P}_{\text{GUS},2}^{\text{FPA}} = \mathbb{P} \left[ \hat{\tau}_2 < |h_2|^2 < \hat{\tau}_2 + \frac{1}{2}\hat{\gamma}_2\hat{\tau}_2, |h_2|^2 < |h_1|^2 < \hat{\gamma}_2\hat{\tau}_2 + 2\hat{\tau}_2 - |h_2|^2 \right] + \mathbb{P} [|h_2|^2 < \hat{\tau}_2]. \quad (60)$$

By applying (8) and (33), the outage probability of  $U_2$  can be expressed as

$$\begin{aligned}\mathcal{P}_{\text{GUS},2}^{\text{FPA}} = & K(K-1) \int_{\hat{\tau}_2}^{\hat{\tau}_2 + \frac{1}{2}\hat{\tau}_2\hat{\gamma}_2} [F_{|h|^2}(\hat{\gamma}_2\hat{\tau}_2 + 2\hat{\tau}_2 - x) - F_{|h|^2}(x)] f_{|h|^2}(x) F_{|h|^2}(x)^{K-2} dx \\ & + K F_{|h|^2}(\hat{\tau}_2)^{K-1} - (K-1) F_{|h|^2}(\hat{\tau}_2)^K.\end{aligned}\quad (61)$$

Following the same steps of deriving (24),  $\mathcal{P}_{\text{GUS},2}^{\text{FPA}}$  can be finally expressed as (53). The proof is complete.  $\blacksquare$

When the transmit SNR approaches infinity,  $\hat{\tau}_1$ ,  $\hat{\tau}_2$ ,  $\hat{\tau}_1 + \hat{\tau}_1\hat{\gamma}_1$ , and  $\hat{\tau}_2 + \frac{1}{2}\hat{\tau}_2\hat{\gamma}_2$  approach zero. Then, substituting (39) and (40) into (57) and (61), we can obtain the high SNR approximation of the two users' outage probabilities. Similar with the derivation of Corollary 1, we can derive the following corollary.

*Corollary 3:* When the transmit SNR  $\rho_m \rightarrow \infty$ , the high SNR approximation of  $\mathcal{P}_{\text{GUS},1}^{\text{FPA}}$  and

$\mathcal{P}_{\text{GUS},2}^{\text{FPA}}$  can be expressed as

$$\begin{aligned}\vec{\mathcal{P}}_{\text{GUS},1}^{\text{FPA}} = & K(S_L \hat{\tau}_1)^K \sum_{k_1=0}^{K-1} \binom{K-1}{k_1} \frac{(\hat{\gamma}_1 + 2)^{K-1-k_1} (-1)^{k_1}}{k_1 + 1} [(1 + \hat{\gamma}_1)^{k_1+1} - (1 + \frac{1}{2} \hat{\gamma}_1)^{k_1+1}] \\ & - K \left( \frac{S_L}{\rho_m} \right)^K \sum_{k_2=0}^{K-1} \binom{K-1}{k_2} \frac{\hat{\gamma}_1}{k_2 + 1} (-1)^{K-1-k_2} [(1 + \hat{\gamma}_1)^{k_2+1} - 1] \\ & + (S_L \hat{\tau}_1)^K [(1 + \frac{1}{2} \hat{\gamma}_1)^K - 1] + (S_L \hat{\tau}_1)^K,\end{aligned}\quad (62)$$

and

$$\begin{aligned}\vec{\mathcal{P}}_{\text{GUS},2}^{\text{FPA}} = & K(K-1)(S_L \hat{\tau}_2)^K \left[ \frac{\hat{\gamma}_2 + 2}{K-1} \left( (1 + \frac{1}{2} \hat{\gamma}_2)^{K-1} - 1 \right) - \frac{2}{K} \left( (1 + \frac{1}{2} \hat{\gamma}_2)^K - 1 \right) \right] \\ & + K(S_L \hat{\tau}_2)^{K-1} - (K-1)(S_L \hat{\tau}_2)^K,\end{aligned}\quad (63)$$

respectively.  $U_1$  and  $U_2$  can achieve diversity orders of  $K$  and  $K-1$ , respectively.

### C. Outage Performance Analysis of the CUS Scheme with FPA Strategy

Assuming the users with the largest and the second-largest CDF values are denoted as  $U_i$  and  $U_j$ , respectively. The following theorem shows their outage probability expressions.

*Theorem 4:* In the CUS scheme with FPA strategy, the outage probability of the user with the largest CDF value can be approximated as

$$\begin{aligned}\mathcal{P}_{\text{CUS},i}^{\text{FPA}} = & \mathcal{G}[\hat{\tau}_i, \epsilon_8; F_{X',Y}^{\text{CUS},III}(x, y)] + \mathcal{G}[\epsilon_8, \hat{\tau}_i + \hat{\tau}_i \hat{\gamma}_i; F_{X',Y}^{\text{CUS},II}(x, y)] \\ & - \mathcal{G}[\hat{\tau}_i, \epsilon_{11}; F_{X',Y}^{\text{CUS},I}(x, y)] - \mathcal{G}[\epsilon_{11}, \hat{\tau}_i + \hat{\tau}_i \hat{\gamma}_i; F_{X',Y}^{\text{CUS},II}(x, y)],\end{aligned}\quad (64)$$

if  $R^\alpha > \hat{\gamma}_i$ , otherwise

$$\begin{aligned}\mathcal{P}_{\text{CUS},i}^{\text{FPA}} = & \mathcal{G}[\hat{\tau}_i, \epsilon_7; F_{X',Y}^{\text{CUS},IV}(x, y)] + \mathcal{G}[\epsilon_7, \epsilon_8; F_{X',Y}^{\text{CUS},III}(x, y)] \\ & + \mathcal{G}[\epsilon_8, \epsilon_9; F_{X',Y}^{\text{CUS},II}(x, y)] + \mathcal{G}[\epsilon_9, \hat{\tau}_i + \hat{\tau}_i \hat{\gamma}_i; F_{X',Y}^{\text{CUS},I}(x, y)] \\ & - \mathcal{G}[\hat{\tau}_i, \hat{\tau}_i + \hat{\tau}_i \hat{\gamma}_i; F_{X',Y}^{\text{CUS},I}(x, y)],\end{aligned}\quad (65)$$

where  $\epsilon_7 = \frac{2\hat{\tau}_i + \hat{\tau}_i \hat{\gamma}_i}{R^\alpha + 2}$ ,  $\epsilon_8 = \hat{\tau}_i + \frac{1}{2} \hat{\tau}_i \hat{\gamma}_i$ ,  $\epsilon_9 = \frac{(2\hat{\tau}_i + \hat{\tau}_i \hat{\gamma}_i)(R^\alpha + 1)}{R^\alpha + 2}$ ,  $\epsilon_{10} = \frac{\hat{\tau}_i}{1 - \hat{\gamma}_i}$ , and  $\epsilon_{11} = \frac{(R^\alpha + 1)\hat{\tau}_i}{R^\alpha + 1 - \hat{\gamma}_i}$ .  $F_{X',Y}^{\text{CUS},I}(x, y)$ ,  $F_{X',Y}^{\text{CUS},II}(x, y)$ ,  $F_{X',Y}^{\text{CUS},III}(x, y)$ , and  $F_{X',Y}^{\text{CUS},IV}(x, y)$  represent the partial derivatives of (12), (13), (14), and (15) with respect to  $x$ , respectively. Note that, in (64) and (65),  $y$  should be replaced with  $2\hat{\tau}_i + \hat{\tau}_i \hat{\gamma}_i - x$  for the positive terms, while  $y$  should be substituted with  $\frac{1}{\hat{\gamma}_i}x - \frac{1}{\rho_m}$  for the negative terms.

The outage probability of the user with the second-largest CDF value can be calculated with the results of Theorem 2 by setting  $\hat{\tau}_s = \hat{\tau}_p = \hat{\tau}_j$  and  $\hat{\gamma}_s = \hat{\gamma}_p = \hat{\gamma}_j$ .

*Proof:* Please refer to Appendix C. ■

Similar to the derivation of Corollary 2, we have the following corollary.

*Corollary 4:* In the CUS scheme with FPA strategy, the scheduled two users can achieve diversity orders of  $K$  and  $K - 1$ , respectively.

*Remark 4:* Corollaries 1 - 4 show that the scheduled users in both GUS and CUS schemes can achieve full diversity orders for both CPA and FPA strategies, and the achieved diversity orders are closely related to the total number of users  $K$ . In other words, the uplink RSMA transmission can achieve the same diversity orders as downlink NOMA transmission [29], [34]. Moreover, compared with the schemes that divide all users in the system into two parts [25], [35], [36], the scheduling schemes considered in this paper can achieve higher diversity orders.

## VI. SIMULATION RESULTS AND DISCUSSIONS

In this section, the accuracy of the theoretical analyses and the performance of different transmission schemes are examined through computer simulations. All the simulation results are averaged over  $10^6$  independent trials, and the users are randomly distributed in the coverage area of the BS in each trial. Hereinafter, unless other specified, the simulation parameters are set similar with [37] as  $\alpha = 3.76$ ,  $K = 4$ ,  $R = 500$  m,  $\hat{R}_i = \hat{R}_j = \hat{R}_p = \hat{R}_s = 1$  bps/Hz. The noise power is set as -100 dBm. Since the multinomial theorem is applied in this paper, to simplify the calculation complexity, all the complexity-accuracy tradeoff parameters are set as 10 [29], which is sufficient to maintain the calculation accuracy.

### A. Simulation Results of the CPA Strategy

Fig. 3 compares the users' outage probabilities and admission probabilities of different scheduling schemes with the CPA strategy, where  $\hat{R}_p = \hat{R}_s = 2$  bps/Hz. The newest NOMA transmission with HSIC decoding strategy [38] is used as a benchmark scheme, in which the secondary user's transmit power is tuned for guaranteeing the primary user's QoS. Moreover, the GUS and CUS schemes are compared with the random user scheduling (RUS) scheme in [22]. It can be observed from Fig. 3(a) that for all the scheduling schemes, RSMA can achieve better performance than NOMA, because it can utilize the power more efficiently. More specifically, the received power of the secondary user is restricted by the interference threshold of the primary user for NOMA. However, in RSMA, the secondary user's abundant received power that exceeds the primary user's decoding threshold can be split to transmit more messages.

It can also be observed from Fig. 3(a) that the GUS and RUS schemes achieve the best and the worst outage performance, respectively. That is because the GUS scheme always schedules the

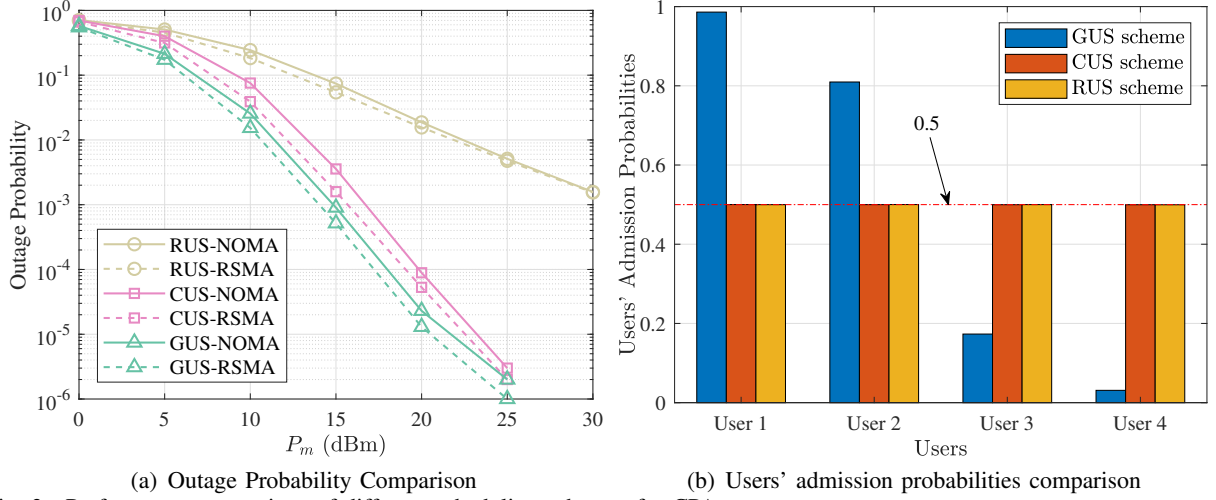


Fig. 3. Performance comparison of different scheduling schemes for CPA strategy.

users with the best channel gains and can effectively employ multi-user diversity, while the users are randomly scheduled in RUS scheme without utilizing multi-user diversity. In order to provide fair access opportunities to the users, the CUS scheme achieves inferior outage probability to the GUS scheme, whereas it can also effectively exploit multi-user diversity. To compare the scheduling fairness performance of the three scheduling schemes, we plot the users' admission probabilities of a 4-user system in Fig. 3(b), where the users' distances to the BS are 100 m, 200 m, 300 m, and 400 m, respectively. We can see that the CUS and RUS schemes can achieve equal admission probability. However, in GUS scheme, the users closer to the BS are scheduled with much higher probability, which leads scheduling unfairness.

Fig. 4 depicts the ergodic data rates of different schemes for CPA strategy, where  $\hat{R}_p = 3$  bps/Hz. It can be observed that RSMA can achieve better ergodic data rate performance than NOMA for all the three scheduling schemes, where such improvement comes from the effective utilization of the secondary user's transmit power. Moreover, the ergodic rate of the GUS scheme is higher than those of the CUS and RUS schemes due to better channel gains of the scheduled users. One interesting phenomenon is that, in the low SNR region, the ergodic data rates of both RSMA and NOMA for each scheduling scheme are identical, and the performance of the GUS scheme is lower than that of both CUS and RUS schemes. That is because when the transmit SNR is low, the primary user may always be in an outage, hence the achievable rates of the secondary users in both RSMA and NOMA schemes are  $\log_2 \left( 1 + \frac{\eta_s}{\eta_p + 1} \right)$ . Moreover, since the secondary user's channel gain of GUS scheme is lower than that of the primary user definitely, and the relationship of the scheduled users' channel gains is not known for both CUS and RUS schemes, which leads to the ergodic rate of GUS scheme is lower than the counterparts.

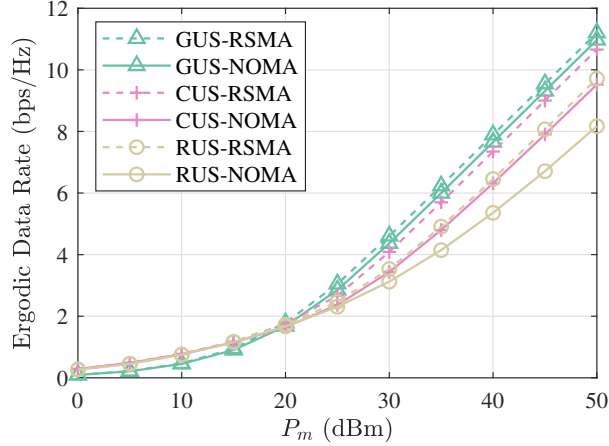


Fig. 4. Ergodic data rate comparison of different schemes for CPA strategy ( $\hat{R}_p = 3$  bps/Hz).

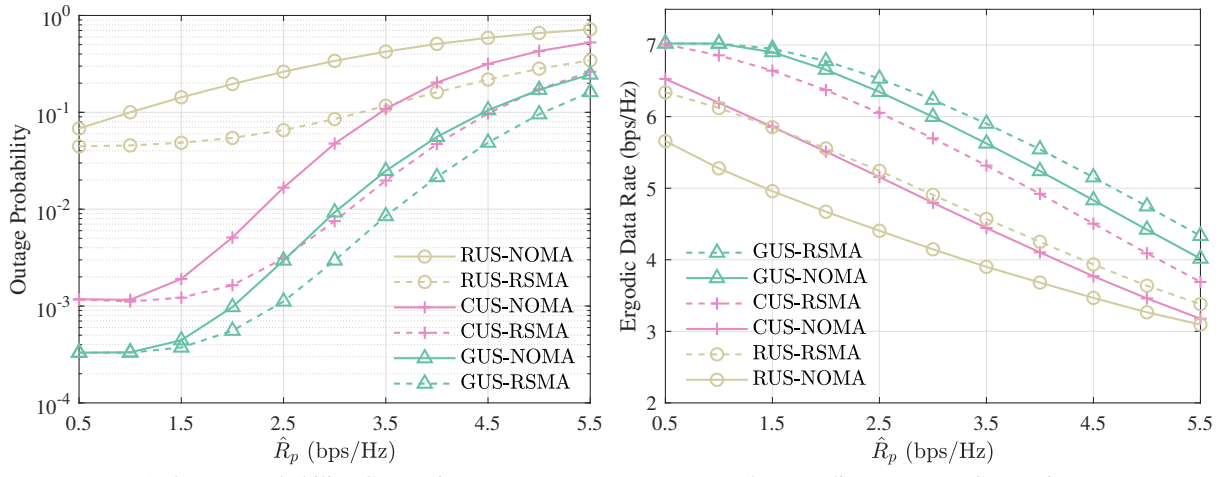


Fig. 5. Performance comparison versus the target rate of  $U_p$  for CPA strategy ( $P_m = 15$  dBm).

In Fig. 5, the outage probability and ergodic data rate performance are compared with a different target rate of  $U_p$ , where  $P_m = 15$  dBm. It can be observed that for all three scheduling strategies, RSMA can achieve better performance than NOMA in most cases. That is because RSMA can utilize the transmit power of  $U_s$  more efficiently by introducing an additional SIC procedure. Moreover, both sub-figures illustrate that the performance of all schemes deteriorates with the uplift of  $\hat{R}_p$ . That is because the sum rates of the two users are fixed for RSMA. Thus, the higher  $\hat{R}_p$  is, the lower rate is reserved for  $U_s$ . For NOMA, the interference threshold of  $U_p$  determines the achievable rate of  $U_s$ , and the interference threshold is decreasing with the increase of  $\hat{R}_p$ .

The accuracy of the developed analytical results for the CPA strategy is examined in Fig. 6, in which the high SNR approximation curve of the GUS-RSMA scheme is obtained based on Corollary 1. The analytical results of GUS-RSMA and CUS-RSMA schemes are plotted based

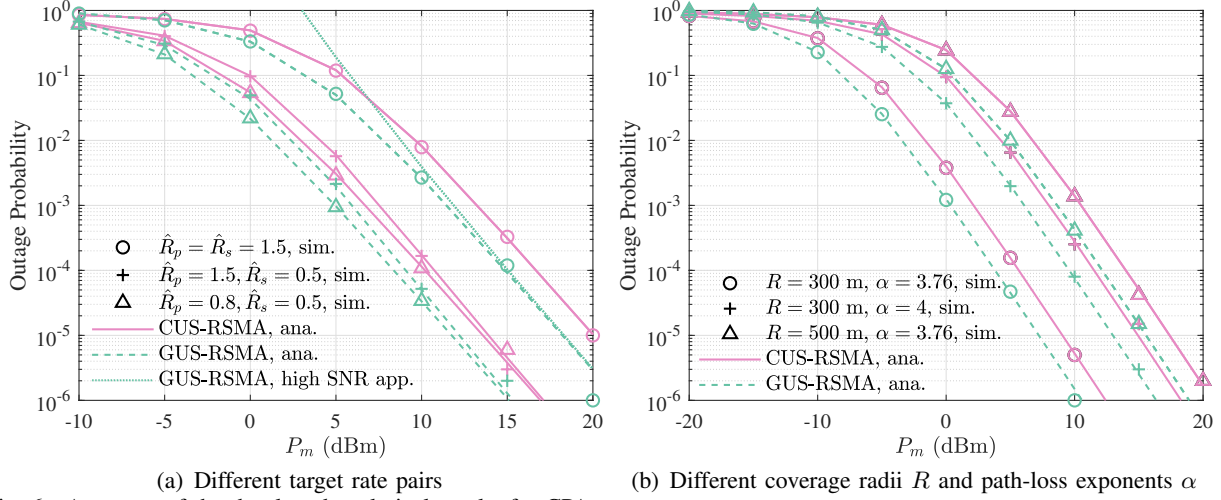


Fig. 6. Accuracy of the developed analytical results for CPA strategy.

on the expressions in Theorems 1 and 2, respectively. The three target rate pairs in Fig. 6(a) correspond to the three cases in Theorem 1. It can be observed that the developed analytical expressions match well with the simulation results in all three cases, which verifies the correctness of the theoretical analyses. Moreover, in the high SNR region, the approximation results of Corollary 1 for the GUS-RSMA scheme also tightly match the simulation results. Note that, for both scheduling schemes, the curves of rate pair “ $\hat{R}_p = 1.5, \hat{R}_s = 0.5$ ” and “ $\hat{R}_p = 0.8, \hat{R}_s = 0.5$ ” coincide in the high SNR region. That can be explained by Corollary 1 that the outage probability in high SNR with lower power is only related to  $K$ ,  $\hat{R}_s$ , and the transmit power, but irrelevant with  $\hat{R}_p$ . In Fig. 6(b), the outage probability is compared with different coverage radii and path-loss exponents for the CPA strategy. It can be seen that the analytical results match well with the simulation results in all cases. Moreover, the outage probabilities of the two scheduling schemes are increasing with the increase of the coverage radius and path-loss exponent. Both result from the severe of the path-loss, which is proportional to the path-loss exponent and scheduled users’ distances to the BS.

### B. Simulation Results of the FPA Strategy

The rate fairness of different schemes are compared in Fig. 7, where the OMA, NOMA, and hybrid NOMA/OMA schemes [39] are used as benchmark schemes. Specifically, for the NOMA scheme, the user with strong channel gain is decoded first to maximize the rate fairness. For the OMA scheme, in order to achieve the same sum rate as the NOMA scheme, the optimal DOF allocation is applied [7], [39], namely, the time-sharing factor for  $U_k$  is  $t_k = \frac{|h_k|^2}{|h_i|^2 + |h_j|^2}$ ,  $k = i, j$ . The hybrid NOMA/OMA scheme [39] always chooses the transmission scheme between NOMA and OMA with higher fairness performance. For the RSMA scheme, the proposed FPA strategy

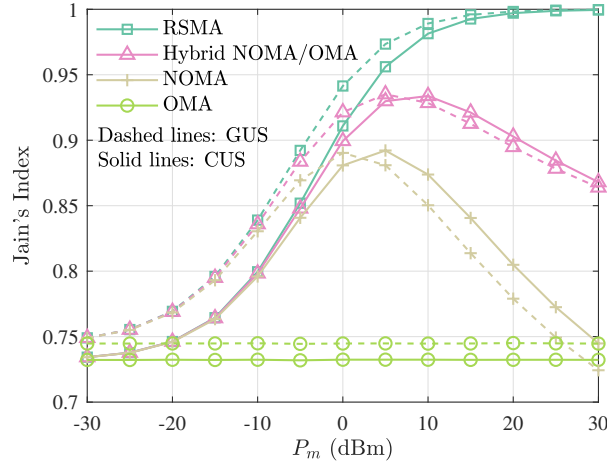


Fig. 7. Rate fairness comparison of different transmission schemes.

is applied. It should be noted that all the four schemes are compared under the condition of achieving the same sum rate.

In the simulations, Jain's index [40] is employed as the metric for rate fairness evaluation, which is widely used as a quantitative fairness measurement and is defined as  $J = \frac{(\sum_{k=1}^K R_k)^2}{K \sum_{k=1}^K (R_k)^2}$ . Note that  $\frac{1}{K} \leq J \leq 1$ , and a larger  $J$  represents a higher fairness level. Particularly, we have  $J = 1$  when all users achieve the same data rate. It can be observed from Fig. 7 that the fairness performance of OMA scheme is constant, which is irrelevant to the transmit power. That is because the achievable rate of  $U_k$  for OMA scheme is  $R_k = t_k R_{sum}$  [7], [39] (where  $R_{sum}$  is the optimal sum rate of uplink MAC), and the Jain's index for OMA scheme is  $J_{OMA} = \frac{R_{sum}^2}{2(t_i^2 R_{sum}^2 + t_j^2 R_{sum}^2)} = \frac{1}{2} + \frac{|h_i|^2 |h_j|^2}{|h_i|^4 + |h_j|^4}$ , which only depends on the users' channel gains. While the fairness performance of both NOMA and hybrid NOMA/OMA schemes increase with the increasing of the transmit power at the beginning, and then deteriorate as the transmit power increasing further. That is because in NOMA scheme, the strong user (with higher received power) is interfered by the weak user (with lower received power), so that the higher the transmit SNR is, the larger interference the strong user will encounter. Therefore, the weak user will achieve a much higher data rate than the strong user in the high SNR region, which greatly degrades the fairness performance of NOMA and hybrid NOMA/OMA schemes. However, the RSMA scheme can always achieve the best fairness performance by adaptively allocating the weak user's total transmit power to two sub-messages, by which the interference to the strong user can be flexibly adjusted.

The CDF of user rate for each transmission scheme is compared in Fig. 8, where  $P_m$  is set as 15 dBm. It can be observed that the user rate distribution of RSMA scheme is more concentrated than those of the other three schemes, which indicates that the RSMA scheme can achieve the best

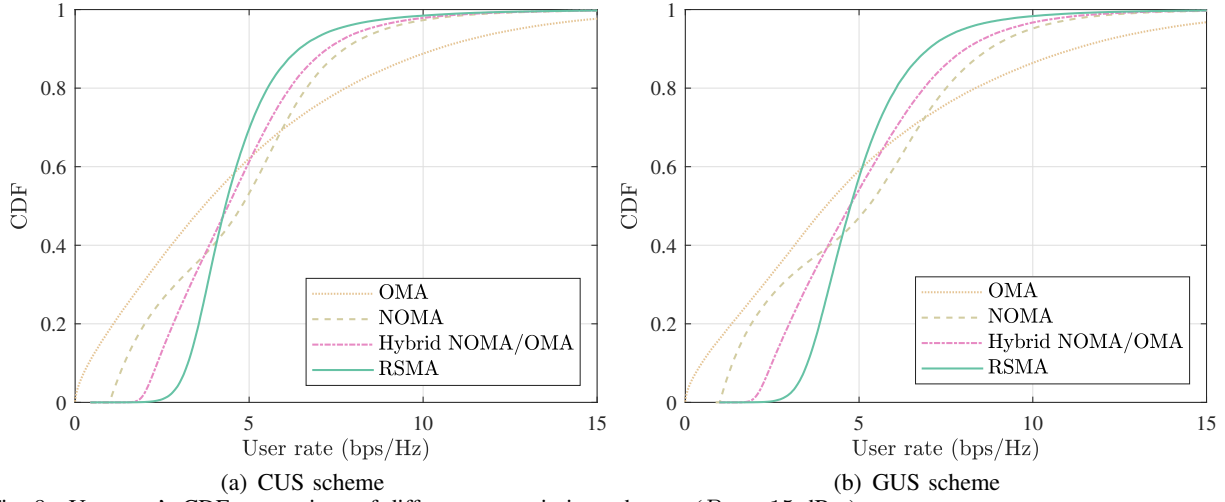


Fig. 8. User rate's CDF comparison of different transmission schemes ( $P_m = 15$  dBm).

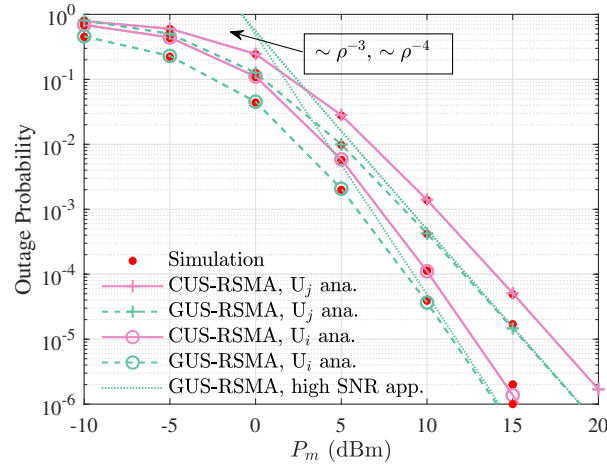


Fig. 9. Accuracy of the developed analytical results for FPA strategy.

fairness performance. Since the 10th-percentile of the user rate is highly related to fairness and user experience [39], we can observe from Fig. 8 that, compared with the hybrid NOMA/OMA scheme, the 10th-percentile of user rate increases by 0.9 bps/Hz (1 bps/Hz) for CUS scheme (GUS scheme). In other words, by combining the proposed FPA strategy with RSMA scheme, the low-rate user's performance and quality of experience can be greatly improved.

Fig. 9 depicts the outage probability versus SNR for GUS-RA-NOMA and CUS-RSMA schemes with FPA policy. It can be observed that the analytical results match well with the simulation results, which verifies the theoretical expressions in Theorems 3 and 4. It can also be observed from Fig. 9 that in the high SNR region, the outage probability curves of  $U_i$  and  $U_j$  are respectively parallel with  $\rho^{-4}$  and  $\rho^{-3}$  for both scheduling schemes, which demonstrates the conclusions of Corollaries 3 and 4 that both schemes can achieve full diversity orders. An interesting observation is that, in the high SNR region, the rate fairness performance of RSMA

scheme is approximate 1 as shown in Fig. 7. However, there is still some probability that  $U_j$  owns extremely low channel gain, leading the outage performance of  $U_j$  inferior to  $U_i$ .

## VII. CONCLUSIONS

In this paper, we studied the outage performance of the uplink RSMA system with randomly deployed users. Specifically, two scheduling schemes were studied, which can maximize the sum rate of opportunistic scheduling with different requirements. Moreover, two kinds of dynamic power allocation strategies were studied, i.e., CPA strategy to guarantee one user's QoS, and FPA strategy to enhance the user's rate fairness, to further explore the flexibility of RSMA. By utilizing stochastic geometry and probability theory, analytical expressions of the users' outage probabilities were derived for each combination of scheduling scheme and power allocation strategy. In addition, we theoretically demonstrated that all schemes can achieve full diversity orders. Simulation results were provided to verify the accuracy of the analytical results and the superior performance of RSMA to NOMA. It is noted that the CUS and GUS schemes can be applied if the operators concern more about the admission fairness and the rate performance, respectively. In the future, we will investigate the performance of multi-cell RSMA with multi-antenna transceivers.

## APPENDIX A PROOF OF LEMMA 1

For given the distances of all users to the BS  $\mathbf{r} = \{r_1, \dots, r_K\}$ , the joint CDF of the scheduled two users' channel gains can be denoted as [34]

$$\begin{aligned}
F_{X,Y}^{\text{CUS}}(x, y | \mathbf{r}) &= \mathbb{P}[X \leq x, Y \leq y | \mathbf{r}] \\
&= \sum_{i=1}^K \sum_{j=1, j \neq i}^K \mathbb{P}[X \leq x, Y \leq y, U_i \text{ and } U_j \text{ have the largest} \\
&\quad \text{and the second-largest CDF values, respectively} | \mathbf{r}] \\
&\stackrel{(a)}{=} \sum_{i=1}^K \sum_{j=1, j \neq i}^K \mathbb{P}[X \leq x, Y \leq y, F_i(X | r_i) \geq F_j(Y | r_j), F_j(Y | r_j) \geq U_k (k \neq i, j)] \\
&= \sum_{i=1}^K \sum_{j=1, j \neq i}^K \int_X \int_Y F_j(Y | r_j)^{K-2} dF_j(Y | r_j) dF_i(X | r_i),
\end{aligned} \tag{A.1}$$

where  $U_k$  in (a) represents the random variable of  $U_k$ 's channel gain's CDF value, which is uniformly distributed in  $[0, 1]$  [31]. In the following, the integral interval will be analyzed first, then the joint CDF will be obtained by averaging over  $r_i$  and  $r_j$ .

### A. Integral Interval Analysis

Firstly, we consider the case  $F_i(x|r_i) > F_j(y|r_j)$ . In this case, for these  $X$  satisfying  $X \geq F_i^{-1}(F_j(y|r_j))$ , all the values of  $Y \leq y$  satisfy the requirement of  $F_i(X|r_i) \geq F_j(Y|r_j)$ , thus the integral interval of  $X$  and  $Y$  are  $[F_i^{-1}(F_j(y|r_j)), x]$  and  $[0, y]$ , respectively; on the other hand, for these  $X < F_i^{-1}(F_j(y|r_j))$ , to meet the requirement of  $F_i(X|r_i) \geq F_j(Y|r_j)$ , the integral interval of  $Y$  should be  $[0, F_j^{-1}(F_i(X|r_i))]$ . Therefore, if  $F_i(x|r_i) > F_j(y|r_j)$ , the joint CDF can be expressed as

$$\begin{aligned} F_{X,Y}^{\text{CUS}}(x, y|\mathbf{r}) &= \sum_{i=1}^K \sum_{j=1, j \neq i}^K \int_{F_i^{-1}(F_j(y|r_j))}^x \int_0^y F_j(Y|r_j)^{K-2} dF_j(Y|r_j) dF_i(X|r_i) \\ &\quad + \sum_{i=1}^K \sum_{j=1, j \neq i}^K \int_0^{F_i^{-1}(F_j(y|r_j))} \int_0^{F_j^{-1}(F_i(X|r_i))} F_j(Y|r_j)^{K-2} dF_j(Y|r_j) dF_i(X|r_i) \\ &= \sum_{i=1}^K \sum_{j=1, j \neq i}^K \frac{1}{K-1} F_j(y|r_j)^{K-1} F_i(x|r_i) - \sum_{i=1}^K \sum_{j=1, j \neq i}^K \frac{1}{K} F_j(y|r_j)^K. \end{aligned} \quad (\text{A.2})$$

For the case  $F_i(x|r_i) \leq F_j(y|r_j)$ , to meet the requirement of  $F_i(X|r_i) \geq F_j(Y|r_j)$ , the integral interval of  $Y$  should be  $[0, F_j^{-1}(F_i(X|r_i))]$  for each  $X \leq x$ . In this case, the joint CDF can be expressed as

$$\begin{aligned} F_{X,Y}^{\text{CUS}}(x, y|\mathbf{r}) &= \sum_{i=1}^K \sum_{j=1, j \neq i}^K \int_0^x \int_0^{F_j^{-1}(F_i(X|r_i))} F_j(Y|r_j)^{K-2} dF_j(Y|r_j) dF_i(X|r_i) \\ &= \sum_{i=1}^K \sum_{j=1, j \neq i}^K \frac{1}{K(K-1)} F_i(x|r_i)^K. \end{aligned} \quad (\text{A.3})$$

### B. Averaging over the Distances

Since all users are randomly distributed in the disc area with radius  $R$ , every user's distance to the BS is independent of each other and the PDF of every user's distance is  $f_{r_k}(z) = \frac{2z}{R^2}$  [41]. Based on that, we can derive the joint CDF by averaging (A.2) and (A.3) over all the distances. Note that, the CDF of  $U_k$  ( $k \in \{1, \dots, K\}$ ) is  $F_k(x|r_k) = 1 - e^{-(1+r_k^\alpha)x}$ . Thus,  $F_i(x|r_i) > F_j(y|r_j)$  means  $(1+r_i^\alpha)x > (1+r_j^\alpha)y$ , which can be converted to  $r_i > [(1+r_j^\alpha)\frac{y}{x} - 1]^{\frac{1}{\alpha}}$ . Note that, when  $r_j \in (0, R)$ , if  $x > y$ ,  $[(1+r_j^\alpha)\frac{y}{x} - 1]^{\frac{1}{\alpha}}$  will be less than  $R$  and it may be even less than 0 (Specially, when  $r_j = (\frac{x}{y} - 1)^{\frac{1}{\alpha}}$ ,  $[(1+r_j^\alpha)\frac{y}{x} - 1]^{\frac{1}{\alpha}} = 0$  holds); on the other hand, if  $x < y$ ,  $[(1+r_j^\alpha)\frac{y}{x} - 1]^{\frac{1}{\alpha}}$  should be larger than 0 and may even larger than  $R$  (Specially, when  $r_j = [(R^\alpha + 1)\frac{x}{y} - 1]^{\frac{1}{\alpha}}$ ,  $[(1+r_j^\alpha)\frac{y}{x} - 1]^{\frac{1}{\alpha}} = R$  holds). For  $F_i(x|r_i) \leq F_j(y|r_j)$ , similar conclusion can be obtained for  $r_i$ . Base on that, the joint CDF can be derived in two cases.

First, we consider the case  $x > y$ . Substituting  $F_k(x|r_k) = 1 - e^{-(1+r_k^\alpha)x}$  into (A.2) and (A.3), the joint CDF can be expressed as

$$\begin{aligned}
F_{X,Y}^{\text{CUS}}(x,y) = & K \int_0^{a_1} \frac{2r_j}{R^2} [1 - e^{-(1+r_j^\alpha)y}]^{K-1} \int_0^R \frac{2r_i}{R^2} [1 - e^{-(1+r_i^\alpha)x}] dr_i dr_j \\
& + K \int_{a_1}^R \frac{2r_j}{R^2} [1 - e^{-(1+r_j^\alpha)y}]^{K-1} \int_{I_1(r_j)}^R \frac{2r_i}{R^2} [1 - e^{-(1+r_i^\alpha)x}] dr_i dr_j \\
& - (K-1) \int_0^{a_1} \frac{2r_j}{R^2} [1 - e^{-(1+r_j^\alpha)y}]^K \int_0^R \frac{2r_i}{R^2} dr_i dr_j \\
& - (K-1) \int_{a_1}^R \frac{2r_j}{R^2} [1 - e^{-(1+r_j^\alpha)y}]^K \int_{I_1(r_j)}^R \frac{2r_i}{R^2} dr_i dr_j \\
& + \int_0^{a_2} \frac{2r_i}{R^2} [1 - e^{-(1+r_i^\alpha)x}]^K \int_{I_2(r_i)}^R \frac{2r_j}{R^2} dr_j dr_i.
\end{aligned} \tag{A.4}$$

It is quite challenging to obtain an insightful expression for (A.4). So, we use Gaussian-Chebyshev quadrature [33] to develop an approximation expression. By applying Gaussian-Chebyshev quadrature and with some manipulations, we can obtain (13).

Note that, (A.4) and (13) require  $a_1 < R$  and  $a_2 > 0$  (namely,  $\frac{x}{y} < R^\alpha + 1$ ). If  $\frac{x}{y} \geq R^\alpha + 1$ , the joint CDF can be simplified to

$$\begin{aligned}
F_{X,Y}^{\text{CUS}}(x,y) = & K \int_0^R \frac{2r_j}{R^2} [1 - e^{-(1+r_j^\alpha)y}]^{K-1} \int_0^R \frac{2r_i}{R^2} [1 - e^{-(1+r_i^\alpha)x}] dr_i dr_j \\
& - (K-1) \int_0^R \frac{2r_j}{R^2} [1 - e^{-(1+r_j^\alpha)y}]^K \int_0^R \frac{2r_i}{R^2} dr_i dr_j.
\end{aligned} \tag{A.5}$$

Similarly, by applying Gaussian-Chebyshev quadrature, we can get (12).

When  $x < y$ , the joint CDF can be denoted as

$$\begin{aligned}
F_{X,Y}^{\text{CUS}}(x,y) = & K \int_0^{a_2} \frac{2r_j}{R^2} [1 - e^{-(1+r_j^\alpha)y}]^{K-1} \int_{I_1(r_j)}^R \frac{2r_i}{R^2} [1 - e^{-(1+r_i^\alpha)x}] dr_i dr_j \\
& - (K-1) \int_0^{a_2} \frac{2r_j}{R^2} [1 - e^{-(1+r_j^\alpha)y}]^K \int_{I_1(r_j)}^R \frac{2r_i}{R^2} dr_i dr_j \\
& + \int_0^{a_1} \frac{2r_i}{R^2} [1 - e^{-(1+r_i^\alpha)x}]^K \int_0^R \frac{2r_j}{R^2} dr_j dr_i \\
& + \int_{a_1}^R \frac{2r_i}{R^2} [1 - e^{-(1+r_i^\alpha)x}]^K \int_{I_2(r_i)}^R \frac{2r_j}{R^2} dr_j dr_i.
\end{aligned} \tag{A.6}$$

Applying Gaussian-Chebyshev quadrature to (A.6), we have (14).

Similar with the case  $x > y$ , (A.6) and (14) require  $\frac{y}{x} < R^\alpha + 1$ . If  $\frac{y}{x} \geq R^\alpha + 1$ , the joint CDF can be simplified as

$$F_{X,Y}^{\text{CUS}}(x,y) = \int_0^R \frac{2r_i}{R^2} [1 - e^{-(1+r_i^\alpha)x}]^K \int_0^R \frac{2r_j}{R^2} dr_j dr_i. \tag{A.7}$$

And we can get (15) by utilizing Gaussian-Chebyshev quadrature as well. The proof of Lemma

1 is completed.

## APPENDIX B PROOF OF THEOREM 2

By applying (23), the outage probability of the second-largest CDF value user with the CPA strategy can be denoted as

$$\begin{aligned}
 \mathcal{P}_{\text{CUS}}^{\text{CPA}} &= F_Y^{\text{CUS}}(\hat{\tau}_s) + \int_{\hat{\tau}_s}^{\hat{\tau}_s(1+\hat{\gamma}_p)} [F_{X,Y'}^{\text{CUS}}(\hat{\tau}_s + \hat{\tau}_p(1+\hat{\gamma}_s) - y, y) - F_{X,Y'}^{\text{CUS}}(\frac{1}{\hat{\gamma}_s}y - \frac{1}{\rho_m}, y)] dy \\
 &= F_Y^{\text{CUS}}(\hat{\tau}_s) + \underbrace{\int_{\hat{\tau}_s}^{\hat{\tau}_s(1+\hat{\gamma}_p)} F_{X,Y'}^{\text{CUS}}(\hat{\tau}_s + \hat{\tau}_p(1+\hat{\gamma}_s) - y, y) dy}_{T_1} \\
 &\quad - \underbrace{\int_{\hat{\tau}_s}^{\hat{\tau}_s(1+\hat{\gamma}_p)} F_{X,Y'}^{\text{CUS}}(\frac{1}{\hat{\gamma}_s}y - \frac{1}{\rho_m}, y) dy}_{T_2},
 \end{aligned} \tag{A.8}$$

where  $F_{X,Y'}^{\text{CUS}}(x, y) = \frac{\partial F_{X,Y'}^{\text{CUS}}(x, y)}{\partial y}$ .  $F_Y^{\text{CUS}}(\hat{\tau}_s)$  can be calculated with (16).

As shown in Remark 1, different values of  $x$  and  $y$  determine which CDF expression should be used. Assume  $\hat{\tau}_s + \hat{\tau}_p(1+\hat{\gamma}_s) - y = y(R^\alpha + 1)$ , we can obtain  $y = \epsilon_1$ . Let  $\hat{\tau}_s + \hat{\tau}_p(1+\hat{\gamma}_s) - y = y$ , we have  $y = \epsilon_2$ . And assuming  $(R^\alpha + 1)(\hat{\tau}_s + \hat{\tau}_p(1+\hat{\gamma}_s) - y) = y$ , we can get  $y = \epsilon_3$ . Note that,  $\epsilon_1$ ,  $\epsilon_2$ , and  $\epsilon_3$  are the points deciding  $\hat{\tau}_s + \hat{\tau}_p(1+\hat{\gamma}_s) - y > y(R^\alpha + 1)$ ,  $y < \hat{\tau}_s + \hat{\tau}_p(1+\hat{\gamma}_s) - y < y(R^\alpha + 1)$ ,  $(\hat{\tau}_s + \hat{\tau}_p(1+\hat{\gamma}_s) - y) < y < (R^\alpha + 1)(\hat{\tau}_s + \hat{\tau}_p(1+\hat{\gamma}_s) - y)$ , and  $(R^\alpha + 1)(\hat{\tau}_s + \hat{\tau}_p(1+\hat{\gamma}_s) - y) < y$ . We can also find that  $\epsilon_1 < \epsilon_2 < \epsilon_3$ . Therefore,  $T_1$  can be calculated with  $F_{X,Y'}^{\text{CUS},\text{I}}(x, y)$ , if  $y < \epsilon_1$ , or with  $F_{X,Y'}^{\text{CUS},\text{II}}(x, y)$  if  $\epsilon_1 < y < \epsilon_2$ , or with  $F_{X,Y'}^{\text{CUS},\text{III}}(x, y)$  if  $\epsilon_2 < y < \epsilon_3$ , or 0 if  $y > \epsilon_3$ . We can see from the above analysis that, it is quite involved to obtain a closed-form expression for (A.8) with the joint CDFs in Lemma 1. To simplify the calculation process, we first calculate  $T_1$  in (A.8). In the following, we will derive  $T_1$  with three cases based on the values of  $\epsilon_2$ ,  $\hat{\tau}_s$ , and  $\hat{\tau}_s(1+\hat{\gamma}_p)$ .

Firstly, we assume  $\epsilon_2 > \hat{\tau}_s(1+\hat{\gamma}_p)$ . In this case,  $T_1$  can be calculated with the following three sub-cases:

1) if  $\epsilon_1 > \hat{\tau}_s(1+\hat{\gamma}_p)$ : We can derive that  $\hat{\tau}_s + \hat{\tau}_p(1+\hat{\gamma}_s) - y > (R^\alpha + 1)y$  for all  $y \in (\hat{\tau}_s, \hat{\tau}_s(1+\hat{\gamma}_p))$ .

Then, substituting  $F_{X,Y'}^{\text{CUS},\text{I}}(x, y)$  to  $T_1$  and applying Gaussian-Chebyshev quadrature, we have

$$T_1 = \mathcal{G}[\hat{\tau}_s, \hat{\tau}_s(1+\hat{\gamma}_p); F_{X,Y'}^{\text{CUS},\text{I}}(x, y)];$$

2) if  $\hat{\tau}_s < \epsilon_1 < \hat{\tau}_s(1+\hat{\gamma}_p)$ : We have  $\hat{\tau}_s + \hat{\tau}_p(1+\hat{\gamma}_s) - y > (R^\alpha + 1)y$  for  $y \in (\hat{\tau}_s, \epsilon_1)$ ,

and  $y < \hat{\tau}_s + \hat{\tau}_p(1+\hat{\gamma}_s) - y < (R^\alpha + 1)y$  for  $y \in (\epsilon_1, \hat{\tau}_s(1+\hat{\gamma}_p))$ . Hence, substituting

$F_{X,Y'}^{\text{CUS},\text{I}}(x, y)$  ( $F_{X,Y'}^{\text{CUS},\text{II}}(x, y)$ ) to  $T_1$  in integral region  $(\hat{\tau}_s, \epsilon_1)$  ( $\epsilon_1, \hat{\tau}_s(1+\hat{\gamma}_p)$ ) and applying

Gaussian-Chebyshev quadrature, we can get  $T_1 = \mathcal{G}[\hat{\tau}_s, \epsilon_1; F_{X,Y'}^{\text{CUS,I}}(x, y)] + \mathcal{G}[\epsilon_1, \hat{\tau}_s(1 + \hat{\gamma}_p); F_{X,Y'}^{\text{CUS,II}}(x, y)]$ ;

3) if  $\epsilon_1 < \hat{\tau}_s$ : We know that  $y < \hat{\tau}_s + \hat{\tau}_p(1 + \hat{\gamma}_s) - y < (R^\alpha + 1)y$  for all  $y \in (\hat{\tau}_s, \hat{\tau}_s(1 + \hat{\gamma}_p))$ .

Similarly, substituting  $F_{X,Y'}^{\text{CUS,II}}(x, y)$  to  $T_1$  and applying Gaussian-Chebyshev quadrature, we can obtain  $T_1 = \mathcal{G}[\hat{\tau}_s, \hat{\tau}_s(1 + \hat{\gamma}_p); F_{X,Y'}^{\text{CUS,II}}(x, y)]$ ;

Then, assuming  $\hat{\tau}_s < \epsilon_2 < \hat{\tau}_s(1 + \hat{\gamma}_p)$ ,  $T_1$  can be calculated with the following four sub-cases:

- 1) if  $\epsilon_1 < \hat{\tau}_s$  and  $\epsilon_3 < \hat{\tau}_s(1 + \hat{\gamma}_p)$ : We can derive that  $y < \hat{\tau}_s + \hat{\tau}_p(1 + \hat{\gamma}_s) - y < (R^\alpha + 1)y$  for  $y \in (\hat{\tau}_s, \epsilon_2)$ ,  $\hat{\tau}_s + \hat{\tau}_p(1 + \hat{\gamma}_s) - y < y < (R^\alpha + 1)(\hat{\tau}_s + \hat{\tau}_p(1 + \hat{\gamma}_s) - y)$  for  $y \in (\epsilon_2, \epsilon_3)$ , and  $y > (R^\alpha + 1)(\hat{\tau}_s + \hat{\tau}_p(1 + \hat{\gamma}_s) - y)$  for  $y \in (\epsilon_3, \hat{\tau}_s(1 + \hat{\gamma}_p))$ ;
- 2) if  $\epsilon_1 < \hat{\tau}_s$  and  $\epsilon_3 > \hat{\tau}_s(1 + \hat{\gamma}_p)$ : We have  $y < \hat{\tau}_s + \hat{\tau}_p(1 + \hat{\gamma}_s) - y < (R^\alpha + 1)y$  for  $y \in (\hat{\tau}_s, \epsilon_2)$  and  $\hat{\tau}_s + \hat{\tau}_p(1 + \hat{\gamma}_s) - y < y < (R^\alpha + 1)(\hat{\tau}_s + \hat{\tau}_p(1 + \hat{\gamma}_s) - y)$  for  $y \in (\epsilon_2, \hat{\tau}_s(1 + \hat{\gamma}_p))$ ;
- 3) if  $\hat{\tau}_s < \epsilon_1 < \epsilon_2$  and  $\epsilon_3 < \hat{\tau}_s(1 + \hat{\gamma}_p)$ : Thus  $\hat{\tau}_s + \hat{\tau}_p(1 + \hat{\gamma}_s) - y > (R^\alpha + 1)y$  for  $y \in (\hat{\tau}_s, \epsilon_1)$ ,  $y < \hat{\tau}_s + \hat{\tau}_p(1 + \hat{\gamma}_s) - y < (R^\alpha + 1)y$  for  $y \in (\epsilon_1, \epsilon_2)$ ,  $\hat{\tau}_s + \hat{\tau}_p(1 + \hat{\gamma}_s) - y < y < (R^\alpha + 1)(\hat{\tau}_s + \hat{\tau}_p(1 + \hat{\gamma}_s) - y)$  for  $y \in (\epsilon_2, \epsilon_3)$ , and  $y > (R^\alpha + 1)(\hat{\tau}_s + \hat{\tau}_p(1 + \hat{\gamma}_s) - y)$  for  $y \in (\epsilon_3, \hat{\tau}_s(1 + \hat{\gamma}_p))$ ;
- 4) if  $\hat{\tau}_s < \epsilon_1 < \epsilon_2$  and  $\epsilon_3 > \hat{\tau}_s(1 + \hat{\gamma}_p)$ : Therefore,  $\hat{\tau}_s + \hat{\tau}_p(1 + \hat{\gamma}_s) - y > (R^\alpha + 1)y$  for  $y \in (\hat{\tau}_s, \epsilon_1)$ ,  $y < \hat{\tau}_s + \hat{\tau}_p(1 + \hat{\gamma}_s) - y < (R^\alpha + 1)y$  for  $y \in (\epsilon_1, \epsilon_2)$ ,  $\hat{\tau}_s + \hat{\tau}_p(1 + \hat{\gamma}_s) - y < y < (R^\alpha + 1)(\hat{\tau}_s + \hat{\tau}_p(1 + \hat{\gamma}_s) - y)$  for  $y \in (\epsilon_2, \hat{\tau}_s(1 + \hat{\gamma}_p))$ .

At last, if  $\epsilon_2 < \hat{\tau}_s$ ,  $T_1$  can be calculated with the following three sub-cases:

- 1) if  $\epsilon_3 < \hat{\tau}_s$ : We have  $y > (R^\alpha + 1)(\hat{\tau}_s + \hat{\tau}_p(1 + \hat{\gamma}_s) - y)$  for  $y \in (\hat{\tau}_s, \hat{\tau}_s(1 + \hat{\gamma}_p))$ ;
- 2) if  $\hat{\tau}_s < \epsilon_3 < \hat{\tau}_s(1 + \hat{\gamma}_p)$ : Then  $\hat{\tau}_s + \hat{\tau}_p(1 + \hat{\gamma}_s) - y < y < (R^\alpha + 1)(\hat{\tau}_s + \hat{\tau}_p(1 + \hat{\gamma}_s) - y)$  for  $y \in (\hat{\tau}_s, \epsilon_3)$  and  $y > (R^\alpha + 1)(\hat{\tau}_s + \hat{\tau}_p(1 + \hat{\gamma}_s) - y)$  for  $y \in (\epsilon_3, \hat{\tau}_s(1 + \hat{\gamma}_p))$ ;
- 3) if  $\epsilon_3 > \hat{\tau}_s(1 + \hat{\gamma}_p)$ : Hence,  $\hat{\tau}_s + \hat{\tau}_p(1 + \hat{\gamma}_s) - y < y < (R^\alpha + 1)\hat{\tau}_s + \hat{\tau}_p(1 + \hat{\gamma}_s) - y$  for  $y \in (\hat{\tau}_s, \hat{\tau}_s(1 + \hat{\gamma}_p))$ .

Combining the above results and applying Gaussian-Chebyshev quadrature, we can obtain Table I.

Now we begin to calculate  $T_2$ . Let  $\frac{1}{\hat{\gamma}_s}y - \frac{1}{\rho_m} = y(R^\alpha + 1)$ , we can get  $y = \epsilon_4$ . Assume  $\frac{1}{\hat{\gamma}_s}y - \frac{1}{\rho_m} = y$ , we have  $y = \epsilon_5$ . And let  $(R^\alpha + 1)(\frac{1}{\hat{\gamma}_s}y - \frac{1}{\rho_m}) = y$ , we can get  $y = \epsilon_6$ . Note that,  $\epsilon_4$ ,  $\epsilon_5$ , and  $\epsilon_6$  are the points deciding  $\frac{1}{\hat{\gamma}_s}y - \frac{1}{\rho_m} > y(R^\alpha + 1)$ ,  $y < \frac{1}{\hat{\gamma}_s}y - \frac{1}{\rho_m} < y(R^\alpha + 1)$ ,  $(\frac{1}{\hat{\gamma}_s}y - \frac{1}{\rho_m}) < y < (R^\alpha + 1)(\frac{1}{\hat{\gamma}_s}y - \frac{1}{\rho_m})$ , and  $(R^\alpha + 1)(\frac{1}{\hat{\gamma}_s}y - \frac{1}{\rho_m}) < y$ . Therefore,  $T_2$  can be calculated with  $F_{X,Y'}^{\text{CUS,I}}(x, y)$  if  $y > \epsilon_4$ , or with  $F_{X,Y'}^{\text{CUS,II}}(x, y)$  if  $\epsilon_5 < y < \epsilon_4$ , or with  $F_{X,Y'}^{\text{CUS,III}}(x, y)$

if  $\epsilon_6 < y < \epsilon_5$ , or 0 if  $y < \epsilon_6$ . For ease of calculation, in the following, we will derive  $T_2$  with two cases based on the values of  $\hat{\gamma}_s$ .

Firstly, we consider the case  $\hat{\gamma}_s > 1$ , and in this case,  $\frac{1}{\hat{\gamma}_s}y - \frac{1}{\rho_m} < y$  always holds. Furthermore, we can derive that, if  $R^\alpha + 1 < \hat{\gamma}_s$ ,  $y > (R^\alpha + 1)(\frac{1}{\hat{\gamma}_s}y - \frac{1}{\rho_m})$  always holds. In this case,  $T_2 = 0$ , since the partial derivative of (15) with respect to  $y$  is 0. On the other hand, if  $R^\alpha + 1 > \hat{\gamma}_s$  and  $y < \epsilon_6$ ,  $y > (R^\alpha + 1)(\frac{1}{\hat{\gamma}_s}y - \frac{1}{\rho_m})$  holds. Hence, we have  $T_2 = 0$  if  $R^\alpha + 1 > \hat{\gamma}_s$  and  $\epsilon_6 > \hat{\tau}_s(1 + \hat{\gamma}_p)$ , and  $T_2 = \mathcal{G}[\epsilon_6, \hat{\tau}_s(1 + \hat{\gamma}_p); F_{X,Y'}^{\text{CUS,III}}(x, y)]$  if  $R^\alpha + 1 > \hat{\gamma}_s$  and  $\epsilon_6 < \hat{\tau}_s(1 + \hat{\gamma}_p)$ .

Now, we consider the case  $\hat{\gamma}_s < 1$ . With some manipulations, we find that  $\frac{1}{\hat{\gamma}_s}y - \frac{1}{\rho_m} > y$  holds when  $y > \epsilon_5$ , and vice versa. Since  $\epsilon_5 > \hat{\tau}_s$ , we will calculate  $T_2$  with two sub-cases according to the values of  $\epsilon_5$  and  $\hat{\tau}_s(1 + \hat{\gamma}_p)$ .

The first sub-case is  $\epsilon_5 < \hat{\tau}_s(1 + \hat{\gamma}_p)$ , namely,  $\hat{\gamma}_s < \frac{\hat{\gamma}_p}{1 + \hat{\gamma}_p}$ . We first calculate the part of  $T_2$  with integral region  $y \in (\hat{\tau}_s, \epsilon_5)$ , represented as  $T_2(\hat{\tau}_s, \epsilon_5)$ . Since  $\hat{\tau}_s < \epsilon_6 < \epsilon_5$ , we have  $T_2(\hat{\tau}_s, \epsilon_5) = \mathcal{G}[\epsilon_6, \epsilon_5; F_{X,Y'}^{\text{CUS,III}}(x, y)]$ . Now, we begin to calculate  $T_2(\epsilon_5, \hat{\tau}_s(1 + \hat{\gamma}_p))$ . With some manipulations, we have the following observations.

- 1) When  $\hat{\gamma}_s > \frac{1}{R^\alpha + 1}$ ,  $\frac{1}{\hat{\gamma}_s}y - \frac{1}{\rho_m} < (R^\alpha + 1)y$  always holds. Thus  $y < \frac{1}{\hat{\gamma}_s}y - \frac{1}{\rho_m} < (R^\alpha + 1)y$  for  $y \in (\epsilon_5, \hat{\tau}_s(1 + \hat{\gamma}_p))$ , namely,  $T_2(\epsilon_5, \hat{\tau}_s(1 + \hat{\gamma}_p)) = \mathcal{G}[\epsilon_5, \hat{\tau}_s(1 + \hat{\gamma}_p); F_{X,Y'}^{\text{CUS,II}}(x, y)]$ .
- 2) When  $\frac{1}{(R^\alpha + 1)(\hat{\gamma}_p + 1)} < \hat{\gamma}_s < \frac{1}{R^\alpha + 1}$ ,  $y < \frac{1}{\hat{\gamma}_s}y - \frac{1}{\rho_m} < (R^\alpha + 1)y$  holds for  $y \in (\epsilon_5, \hat{\tau}_s(1 + \hat{\gamma}_p))$  as well, namely,  $T_2(\epsilon_5, \hat{\tau}_s(1 + \hat{\gamma}_p)) = \mathcal{G}[\epsilon_5, \hat{\tau}_s(1 + \hat{\gamma}_p); F_{X,Y'}^{\text{CUS,II}}(x, y)]$ .
- 3) When  $\hat{\gamma}_s < \frac{1}{(R^\alpha + 1)(\hat{\gamma}_p + 1)}$ ,  $y < \frac{1}{\hat{\gamma}_s}y - \frac{1}{\rho_m} < (R^\alpha + 1)y$  holds for  $y \in (\epsilon_5, \epsilon_4)$  and  $\frac{1}{\hat{\gamma}_s}y - \frac{1}{\rho_m} > (R^\alpha + 1)y$  holds for  $y \in (\epsilon_4, \hat{\tau}_s(1 + \hat{\gamma}_p))$ , namely,  $T_2(\epsilon_5, \hat{\tau}_s(1 + \hat{\gamma}_p)) = \mathcal{G}[\epsilon_5, \epsilon_4; F_{X,Y'}^{\text{CUS,II}}(x, y)] + \mathcal{G}[\epsilon_4, \hat{\tau}_s(1 + \hat{\gamma}_p); F_{X,Y'}^{\text{CUS,I}}(x, y)]$ .

The second sub-case is  $\epsilon_5 > \hat{\tau}_s(1 + \hat{\gamma}_p)$ , namely,  $\hat{\gamma}_s > \frac{\hat{\gamma}_p}{1 + \hat{\gamma}_p}$ . In this case, if  $\epsilon_6 > \hat{\tau}_s(1 + \hat{\gamma}_p)$  (namely,  $\hat{\gamma}_s > \frac{(R^\alpha + 1)\hat{\gamma}_p}{1 + \hat{\gamma}_p}$ ), we have  $y > (\frac{1}{\hat{\gamma}_s}y - \frac{1}{\rho_m})(R^\alpha + 1)$ , thus  $T_2 = 0$ . On the other hand, if  $\hat{\gamma}_s < \frac{(R^\alpha + 1)\hat{\gamma}_p}{1 + \hat{\gamma}_p}$ , we have  $y > (\frac{1}{\hat{\gamma}_s}y - \frac{1}{\rho_m})(R^\alpha + 1)$  for  $y \in (\hat{\tau}_s, \epsilon_6)$  and  $\frac{1}{\hat{\gamma}_s}y - \frac{1}{\rho_m} < y < (\frac{1}{\hat{\gamma}_s}y - \frac{1}{\rho_m})(R^\alpha + 1)$  for  $y \in (\epsilon_6, \hat{\tau}_s(1 + \hat{\gamma}_p))$ . Which means  $T_2 = \mathcal{G}[\epsilon_6, \hat{\tau}_s(1 + \hat{\gamma}_p); F_{X,Y'}^{\text{CUS,III}}(x, y)]$ . Combine the above results, we can obtain Table II. The proof of Theorem 2 is completed.

APPENDIX C  
PROOF OF THEOREM 4

By applying (49), the outage probability of the user with the largest CDF value in fairness-oriented power allocation scheme can be denoted as

$$\begin{aligned}
 \mathcal{P}_{\text{CUS}}^{\text{FPA}} &= F_X^{\text{CUS}}(\hat{\tau}_i) + \int_{\hat{\tau}_i}^{\hat{\tau}_i(1+\hat{\gamma}_i)} [F_{X',Y}^{\text{CUS}}(x, 2\hat{\tau}_i + \hat{\tau}_i\hat{\gamma}_i - x) - F_{X',Y}^{\text{CUS}}(x, \frac{1}{\hat{\gamma}_i}x - \frac{1}{\rho_m})]dx \\
 &= F_X^{\text{CUS}}(\hat{\tau}_i) + \underbrace{\int_{\hat{\tau}_i}^{\hat{\tau}_i(1+\hat{\gamma}_i)} F_{X',Y}^{\text{CUS}}(x, 2\hat{\tau}_i + \hat{\tau}_i\hat{\gamma}_i - x)dx}_{T_3} \\
 &\quad - \underbrace{\int_{\hat{\tau}_i}^{\hat{\tau}_i(1+\hat{\gamma}_i)} F_{X',Y}^{\text{CUS}}(x, \frac{1}{\hat{\gamma}_i}x - \frac{1}{\rho_m})dx}_{T_4},
 \end{aligned} \tag{A.9}$$

where  $F_{X',Y}^{\text{CUS}}(x, y) = \frac{\partial F_{X',Y}^{\text{CUS}}(x,y)}{\partial x}$ . Note that,  $F_X^{\text{CUS}}(\hat{\tau}_i)$  in (A.9) can be calculated with (15).

In the following, we will derive  $T_3$  first, where  $y = 2\hat{\tau}_i + \hat{\tau}_i\hat{\gamma}_i - x$ . When  $x(R^\alpha + 1) = 2\hat{\tau}_i + \hat{\tau}_i\hat{\gamma}_i - x$ , we have  $x = \epsilon_7$ ; let  $x = 2\hat{\tau}_i + \hat{\tau}_i\hat{\gamma}_i - x$ , we have  $x = \epsilon_8$ ; and when  $x = (R^\alpha + 1)(2\hat{\tau}_i + \hat{\tau}_i\hat{\gamma}_i - x)$ , we can get  $x = \epsilon_9$ . Note that,  $\epsilon_7 < \epsilon_8 < \epsilon_9$ . Since  $\hat{\tau}_i < \epsilon_8 < \hat{\tau}_i + \hat{\tau}_i\hat{\gamma}_i$ , the calculation of  $T_3$  can be divided into two parts, namely,  $T_3(\hat{\tau}_i, \epsilon_8)$  and  $T_3(\epsilon_8, \hat{\tau}_i + \hat{\tau}_i\hat{\gamma}_i)$ .

Let us derive  $T_3(\hat{\tau}_i, \epsilon_8)$  first, which can be calculated with the following two cases:

- 1) if  $\epsilon_7 < \hat{\tau}_i$  (namely,  $R^\alpha > \hat{\gamma}_i$ ): We have  $x < 2\hat{\tau}_i + \hat{\tau}_i\hat{\gamma}_i - x < x(R^\alpha + 1)$  for  $x \in (\hat{\tau}_i, \epsilon_8)$ .
- 2) if  $\epsilon_7 > \hat{\tau}_i$  (namely,  $R^\alpha < \hat{\gamma}_i$ ): We have  $2\hat{\tau}_i + \hat{\tau}_i\hat{\gamma}_i - x > x(R^\alpha + 1)$  for  $x \in (\hat{\tau}_i, \epsilon_7)$ , and  $x < 2\hat{\tau}_i + \hat{\tau}_i\hat{\gamma}_i - x < x(R^\alpha + 1)$  holds for  $x \in (\epsilon_7, \epsilon_8)$ .

Similarly, the calculation of  $T_3(\epsilon_8, \hat{\tau}_i + \hat{\tau}_i\hat{\gamma}_i)$  can also be divided into two cases:

- 1) if  $\epsilon_9 > \hat{\tau}_i(1 + \hat{\gamma}_i)$  (namely,  $R^\alpha > \hat{\gamma}_i$ ): We have  $(2\hat{\tau}_i + \hat{\tau}_i\hat{\gamma}_i - x)(R^\alpha + 1) > x > 2\hat{\tau}_i + \hat{\tau}_i\hat{\gamma}_i - x$  for  $x \in (\epsilon_8, \hat{\tau}_i + \hat{\tau}_i\hat{\gamma}_i)$ .
- 2) if  $\epsilon_9 < \hat{\tau}_i(1 + \hat{\gamma}_i)$  (namely,  $R^\alpha < \hat{\gamma}_i$ ): We have  $2\hat{\tau}_i + \hat{\tau}_i\hat{\gamma}_i - x < x < (2\hat{\tau}_i + \hat{\tau}_i\hat{\gamma}_i - x)(R^\alpha + 1)$  for  $x \in (\epsilon_8, \epsilon_9)$ , and  $x > (2\hat{\tau}_i + \hat{\tau}_i\hat{\gamma}_i - x)(R^\alpha + 1)$  holds for  $x \in (\epsilon_9, \hat{\tau}_i + \hat{\tau}_i\hat{\gamma}_i)$ .

In the following, we will derive  $T_4$ , where  $y = \frac{1}{\hat{\gamma}_i}x - \frac{1}{\rho_m}$ . After some manipulations, we can find that  $x = \frac{1}{\hat{\gamma}_i}x - \frac{1}{\rho_m}$  holds, if  $x = \epsilon_{10}$ . Since  $\epsilon_{10} > \hat{\tau}_i + \hat{\tau}_i\hat{\gamma}_i$ , we know that  $x > \frac{1}{\hat{\gamma}_i}x - \frac{1}{\rho_m}$  always holds for all  $x \in (\hat{\tau}_i, \hat{\tau}_i + \hat{\tau}_i\hat{\gamma}_i)$ . Moreover, we know that,  $x = (R^\alpha + 1) \left( \frac{1}{\hat{\gamma}_i}x - \frac{1}{\rho_m} \right)$  holds when  $x = \epsilon_{11}$ , and  $\epsilon_{11} > \hat{\tau}_i$ . Thus,  $T_4$  can be calculated in the following two cases:

- 1) if  $\epsilon_{11} < \hat{\tau}_i(1 + \hat{\gamma}_i)$  (namely,  $R^\alpha > \hat{\gamma}_i$ ): We have  $x > \left( \frac{1}{\hat{\gamma}_i}x - \frac{1}{\rho_m} \right)(R^\alpha + 1)$  for  $x \in (\hat{\tau}_i, \epsilon_{11})$ , and  $\frac{1}{\hat{\gamma}_i}x - \frac{1}{\rho_m} < x < \left( \frac{1}{\hat{\gamma}_i}x - \frac{1}{\rho_m} \right)(R^\alpha + 1)$  holds for  $x \in (\epsilon_{11}, \hat{\tau}_i + \hat{\tau}_i\hat{\gamma}_i)$ .

2) if  $\epsilon_{11} > \hat{\tau}_i(1 + \hat{\gamma}_i)$  (namely,  $R^\alpha < \hat{\gamma}_i$ ): We have  $x > \left(\frac{1}{\hat{\gamma}_i}x - \frac{1}{\rho_m}\right)(R^\alpha + 1)$  for all  $x \in (\hat{\tau}_i, \hat{\tau}_i + \hat{\tau}_i\hat{\gamma}_i)$ .

Finally, combining all the above results and applying Gaussian-Chebyshev quadrature, we can get (64) and (65). It can be observed that (51) is a special case of (23), hence the outage probability of the user with the second largest CDF value in fairness-oriented power allocation scheme can be calculated with the results of Theorem 2. The proof of Theorem 4 is completed.

## REFERENCES

- [1] B. Clerckx, H. Joudeh, C. Hao, M. Dai, and B. Rassouli, “Rate splitting for MIMO wireless networks: A promising PHY-layer strategy for LTE evolution,” *IEEE Commun. Mag.*, vol. 54, no. 5, pp. 98–105, May 2016.
- [2] Y. Mao *et al.*, “Rate-splitting multiple access for downlink communication systems: Bridging, generalizing, and outperforming SDMA and NOMA,” *EURASIP J. Wireless Commun. Netw.*, vol. 2018, no. 1, pp. 1–54, May 2018.
- [3] Z. Ding *et al.*, “A survey on non-orthogonal multiple access for 5G networks: Research challenges and future trends,” *IEEE J. Sel. Areas Commun.*, vol. 35, no. 10, pp. 2181–2195, Oct. 2017.
- [4] H. Cao, J. Cai, S. Huang, and Y. Lu, “Online adaptive transmission strategy for buffer-aided cooperative NOMA systems,” *IEEE Trans. Mobile Comput.*, vol. 18, no. 5, pp. 1133–1144, May 2019.
- [5] Y. Mao, B. Clerckx, and V. O. K. Li, “Rate-splitting for multiantenna non-orthogonal unicast and multicast transmission: Spectral and energy efficiency analysis,” *IEEE Trans. Commun.*, vol. 67, no. 12, pp. 8754–8770, Dec. 2019.
- [6] B. Rimoldi and R. Urbanke, “A rate-splitting approach to the Gaussian multiple-access channel,” *IEEE Trans. Inf. Theory*, vol. 42, no. 2, pp. 364–375, Mar. 1996.
- [7] D. Tse and P. Viswanath, *Fundamentals of Wireless Communication*. Cambridge, U.K.: Cambridge Univ. Press, 2005.
- [8] Y. Zhu, Z. Zhang, X. Wang, and X. Liang, “A low-complexity nonorthogonal multiple access system based on rate splitting,” in *Proc. 9th Int. Conf. Wireless Commun. Signal Process. (WCSP)*, Oct. 2017, pp. 1–6.
- [9] H. Joudeh and B. Clerckx, “Sum-rate maximization for linearly precoded downlink multiuser MISO systems with partial CSIT: A rate-splitting approach,” *IEEE Trans. Commun.*, vol. 64, no. 11, pp. 4847–4861, Nov. 2016.
- [10] B. Clerckx *et al.*, “Rate-splitting unifying SDMA, OMA, NOMA, and multicasting in MISO broadcast channel: A simple two-user rate analysis,” *IEEE Wireless Commun. Lett.*, vol. 9, no. 3, pp. 349–353, Mar. 2020.
- [11] Z. Yang, M. Chen, W. Saad, and M. Shikh-Bahaei, “Optimization of rate allocation and power control for rate splitting multiple access (RSMA),” *IEEE Trans. Commun.*, vol. 69, no. 9, pp. 5988–6002, Sep. 2021.
- [12] J. Zeng, T. Lv, W. Ni, R. P. Liu, N. C. Beaulieu, and Y. J. Guo, “Ensuring max–min fairness of UL SIMO-NOMA: A rate splitting approach,” *IEEE Trans. Veh. Technol.*, vol. 68, no. 11, pp. 11080–11093, Nov. 2019.
- [13] Z. Yang, M. Chen, W. Saad, W. Xu, and M. Shikh-Bahaei, “Sum-rate maximization of uplink rate splitting multiple access (RSMA) communication,” *IEEE Trans. Mobile Comput.*, to be published, doi: 10.1109/TMC.2020.3037374.
- [14] Y. Zhu, X. Wang, Z. Zhang, X. Chen, and Y. Chen, “A rate-splitting nonorthogonal multiple access scheme for uplink transmission,” in *Proc. 9th Int. Conf. Wireless Commun. Signal Process. (WCSP)*, Oct. 2017, pp. 1–6.
- [15] H. Liu, T. A. Tsiftsis, K. J. Kim, K. S. Kwak, and H. V. Poor, “Rate splitting for uplink NOMA with enhanced fairness and outage performance,” *IEEE Trans. Wireless Commun.*, vol. 19, no. 7, pp. 4657–4670, Jul. 2020.
- [16] O. Abbasi and H. Yanikomeroglu, “Transmission Scheme, Detection and Power Allocation for Uplink User Cooperation with NOMA and RSMA,” Jan. 2022. [Online]. Available: <https://arxiv.org/abs/2201.04572>
- [17] S. K. Singh, K. Agrawal, K. Singh and C. -P. Li, “Outage probability and throughput analysis of UAV-assisted rate-splitting multiple access,” *IEEE Wireless Commun. Lett.*, vol. 10, no. 11, pp. 2528–2532, Nov. 2021.
- [18] H. Kong, M. Lin, Z. Wang, J. -Y. Wang, W. -P. Zhu and J. Wang, “Performance analysis for rate splitting uplink NOMA transmission in high throughput satellite systems,” *IEEE Wireless Commun. Lett.*, vol. 11, no. 4, pp. 816–820, Apr. 2022.
- [19] S. A. Tegos, P. D. Diamantoulakis and G. K. Karagiannidis, “On the Performance of Uplink Rate-Splitting Multiple Access,” *IEEE Commun. Lett.*, vol. 26, no. 3, pp. 523–527, Mar. 2022.
- [20] H. Liu, Z. Bai, H. Lei, G. Pan, K. J. Kim and T. Tsiftsis, “A new rate splitting strategy for uplink CR-NOMA systems,” *IEEE Trans. Veh. Technol.*, to be published, doi: 10.1109/TVT.2022.3166218.
- [21] X. Yue, S. A. Tegos, P. D. Diamantoulakis, Z. Ma, G. K. Karagiannidis, “Cognitive radio inspired uplink rate-splitting multiple access,” Apr. 2022. [Online]. Available: <http://arxiv.org/abs/2204.05825>
- [22] E. Demarchou, C. Psomas, and I. Krikidis, “Channel statistics-based rate splitting with spatial randomness,” in *Proc. Int. Conf. Commun. Workshops (ICC Workshops)*, Jun. 2020, pp. 1–6.

- [23] E. Demarchou, C. Psomas and I. Krikidis, "On the sum rate of MISO rate splitting with spatial randomness," in *Proc. Int. Symp. Wireless Commun. Syst. (ISWCS)*, Sep. 2021, pp. 1-5.
- [24] E. Demarchou, C. Psomas and I. Krikidis, "Rate splitting with wireless edge caching: A system-level-based co-design," *IEEE Trans. Commun.*, vol. 70, no. 1, pp. 664-679, Jan. 2022.
- [25] H. Lu, X. Xie, Z. Shi, and J. Cai, "Outage performance of CDF-based scheduling in downlink and uplink NOMA systems," *IEEE Trans. Veh. Technol.*, vol. 69, no. 12, pp. 14945-14959, Dec. 2020.
- [26] M. Haenggi, *Stochastic Geometry for Wireless Networks*. Cambridge, U.K.: Cambridge Univ. Press, 2012.
- [27] L. Zheng and D. N. C. Tse, "Diversity and multiplexing: a fundamental tradeoff in multiple antenna channels," *IEEE Trans. Inf. Theory*, vol. 49, pp. 1073-1096, May 2003.
- [28] H. A. David and H. N. Nagaraja, *Order Statistics*. John Wiley, New York, 3rd ed., 2003.
- [29] Z. Ding, Z. Yang, P. Fan, and H. V. Poor, "On the performance of non-orthogonal multiple access in 5G systems with randomly deployed users," *IEEE Signal Process. Lett.*, vol. 21, no. 12, pp. 1501-1505, Dec. 2014.
- [30] D. Park, H. Seo, H. Kwon, and B. G. Lee, "Wireless packet admitting based on the cumulative distribution function of user transmission rate," *IEEE Trans. Commun.*, vol. 53, no. 11, pp. 1919-1929, Nov. 2005.
- [31] H. Jin *et al.*, "Fundamental limits of CDF-based scheduling: Throughput, fairness, and feedback overhead," *IEEE/ACM Trans. Netw.*, vol. 23, no. 3, pp. 894-907, Jun. 2015.
- [32] Z. Ding, P. Fan, and H. V. Poor, "Impact of user pairing on 5G nonorthogonal multiple-access downlink transmissions," *IEEE Trans. Veh. Technol.*, vol. 65, no. 8, pp. 6010-6023, Aug. 2016.
- [33] E. Hildebrand, *Introduction to Numerical Analysis*. New York, NY, USA: Dover, 1987.
- [34] B. Lim, S. S. Nam, Y.-C. Ko, and M.-S. Alouini, "Outage analysis for downlink non-orthogonal multiple access (NOMA) with CDF-based scheduling," *IEEE Wireless Commun. Lett.*, vol. 9, no. 6, pp. 822-825, Jun. 2020.
- [35] L. Yang *et al.*, "Opportunistic adaptive non-orthogonal multiple access in multiuser wireless systems: Probabilistic user scheduling and performance analysis," *IEEE Trans. Wireless Commun.*, vol. 19, no. 9, pp. 6065-6082, Sep. 2020.
- [36] K. Janghel and S. Prakriya, "Performance of adaptive OMA/cooperative NOMA scheme with user selection," *IEEE Commun. Lett.*, vol. 22, no. 10, pp. 2092-2095, Oct. 2018.
- [37] Z. Wei, L. Yang, D. W. K. Ng, J. Yuan, and L. Hanzo, "On the performance gain of NOMA Over OMA in uplink communication systems," *IEEE Trans. Commun.*, vol. 68, no. 1, pp. 536-568, Jan. 2020.
- [38] Y. Sun, Z. Ding, and X. Dai, "A new design of hybrid SIC for improving transmission robustness in uplink NOMA," *IEEE Trans. Veh. Technol.*, vol. 70, no. 5, pp. 5083-5087, May 2021.
- [39] Z. Wei, J. Guo, D. W. K. Ng, and J. Yuan, "Fairness comparison of uplink NOMA and OMA," in *Proc. IEEE 85th Veh. Technol. Conf. (VTC Spring)*, Jun. 2017, pp. 1-6.
- [40] R. Jain, D. Chiu, and W. Hawe, "A quantitative measure of fairness and discrimination for resource allocation in shared systems" Digit. Equip. Corp., Maynard, MA, USA, Tech. Rep. DEC-TR-301, 1984.
- [41] J. F. C. Kingman, *Poisson Processes*. Oxford, U.K.: Oxford Univ. Press, 1993.